Review

Biosorption of Heavy Metal in Wastewater with Biochar: A Review

Nko Okina Solomon , Donghee Kang , Gbekeloluwa B. Oguntimein *

Posted Date: 22 May 2026

doi: 10.20944/preprints202605.1519.v1

Keywords: biosorption; heavy metal; wastewater; biochar adsorption mechanisms; modification strategies

 doi:10.20944/preprints202605.1519.v1

Review

Biosorption of Heavy Metal in Wastewater with Biochar: A Review

Nko Okina Solomon, Donghee Kang and Gbekeloluwa B. Oguntimein *

Department of Civil and Environmental Engineering, Morgan State University, Baltimore, MD, 21212, USA

* Correspondence: gbeke.oguntimein@morgan.edu (G.B. O.)

Abstract

Biochar, a carbon-rich material produced through pyrolysis of biomass under limited oxygen, offers a potentially sustainable and cost-competitive solution (qualitative assessment; quantitative LCA and techno-economic data are beyond the scope of this review) for the removal of heavy metals from wastewater. Its high porosity, surface area, and surface functional groups enable diverse adsorption mechanisms including complexation, ion exchange, and precipitation. Feedstock selection and production parameters critically influence biochar's physicochemical properties and adsorption performance. Modification techniques such as chemical functionalization, metal impregnation, and composite formation enhance removal efficiency and selectivity for specific contaminants. Applications span industrial, municipal, and agricultural wastewaters, addressing multi-contaminant challenges under variable environmental conditions. Factors affecting removal efficiency include pH, temperature, contaminant concentration, and competing ions, while regeneration methods are essential for maintaining long-term functionality and are discussed. Biochar can be reused and regenerated using bases and acids, but environmental risks related to biochar use, including potential contaminant leaching and ecological impacts, require careful management and regulatory compliance. Future research should focus on novel modification strategies, scaling production for industrial use, and optimizing integration within treatment systems to meet stringent discharge standards and promote sustainable water management.

Keywords: biosorption; heavy metal; wastewater; biochar adsorption mechanisms; modification strategies

1. Introduction

Biochar has attracted considerable scientific interest for its application in wastewater remediation, particularly for the removal of heavy metals. At its core, biochar is a carbon-rich material formed through the pyrolysis of biomass under a limited oxygen supply [1]. This thermal decomposition process yields a solid adsorbent with high porosity and surface area, characteristics that underpin its capacity to bind contaminants from aqueous environments [2]. The feedstocks used in its production range widely, from agricultural residues like straw and sugar beet waste to animal-derived materials, each conferring distinct physicochemical properties that can influence adsorption efficiency [3]. The economic and environmental profile of biochar makes it a compelling alternative to traditional sorbents such as activated carbon. While activated carbon demonstrates impressive adsorption capabilities, its energy-intensive manufacturing processes drive up costs, limiting broader application, particularly in regions with limited resources for such production. Biochar offers a more sustainable pathway, leveraging abundant biomass waste streams that would otherwise contribute to disposal challenges. This utilization transforms waste into a functional resource capable of removing toxic metals such as cadmium, lead, copper, and nickel from contaminated water systems [4]. Furthermore, the renewability of biomass ensures a consistent supply chain without the ecological burden associated with mining or non-renewable raw material extraction [5]. From a performance standpoint, pristine biochar exhibits moderate adsorption potential; however,

 doi:10.20944/preprints202605.1519.v1

modifying its surface chemistry markedly increases efficacy. Adjustments to surface functional groups, pore distribution, and structural morphology enhance the affinity for targeted metal [6]. Approaches to modification include co-doping with metals or non-metals, incorporation of organic moieties, and co-pyrolysis using multiple feedstocks. Such techniques have demonstrated substantial improvements in adsorption efficiency and pollutant selectivity [5].

In certain instances, modified composites significantly surpass unaltered biochar in terms of uptake capacity for specific contaminants. This versatility extends beyond heavy metals. Multiple studies illustrate how biochar successfully removes pharmaceutical pollutants from water, a growing concern due to their persistence and biological impact [6–8]. Its physicochemical properties enable the concurrent elimination of inorganic species and organic micropollutants in intricate wastewater matrices [9]. Despite this wide-ranging applicability, operational challenges remain low surface functionalization in certain feedstocks can limit removal rates; aggregation during application may reduce available active sites; and efficiency under variable pH or ionic strength conditions can vary. Historical reliance on chemical precipitation or ion exchange for heavy metal removal provided baseline treatments but lacked the sustainability advantages inherent to biochar systems [5]. such as reduced environmental impact and improved long-term effectiveness in diverse wastewater conditions. Adsorption has emerged as not only cost-effective but also adaptable across scales, from small, decentralized treatment units to larger municipal facilities. This scalability owes much to biochar's straightforward production routes, such as pyrolysis, hydrothermal carbonization, microwave processing, gasification, and torrefaction [6]. Each method governs yield quality differently: higher pyrolysis temperatures often increase surface area yet may reduce certain oxygen-containing functional groups critical for binding polar contaminants. Adjusting parameters like residence time provides further control over final properties [5].

Variation in feedstock composition introduces another layer of complexity. Comparative studies show that dairy waste-derived biochar may excel at removing lead ions due to electronegativity differences along the char's external surface relative to other sources like sugar beet residue [3]. Similarly, agricultural by-product-derived biochars can closely mimic the properties of activated carbon without incurring comparable production costs [4]. This indicates that selecting an optimal biomass source is highly context-dependent; treatment objectives must align with feedstock characteristics for maximised performance. Environmental scientists increasingly recognise the dual benefit offered by biochar: it mitigates pollution while contributing to resource recovery [10]. Wastewater is recast not merely as a hazard but as a secondary source of recoverable nutrients or energy-bound compounds within integrated management frameworks. Biochar fits neatly into this paradigm by serving simultaneously as an adsorbent and an avenue for recycling carbon-rich residues back into productive use cycles. However, the regenerative aspects, recovering spent biochar for reuse, are yet underexplored beyond short-term laboratory trials [11]. Understanding long-term ageing effects on structure and adsorption capability will be necessary before widespread adoption in commercial operations becomes viable. These points collectively frame biochar as an environmentally responsible option that intersects economic feasibility with effective contaminant removal performance. Whether tackling industrial effluents or addressing diffuse agricultural run-off carrying metals into hydrological networks, this material presents adaptable strategies grounded in accessible technology paths [1]. The challenge lies less in proving efficacy, which numerous lab-scale studies have already established, and more in optimising preparation methods alongside regeneration protocols so that real-world deployments retain both efficiency and affordability over extended lifespans [11].

This review is a narrative synthesis of peer-reviewed literature on the use of biochar for removing heavy metals from wastewater. It seeks to unify knowledge regarding biochar production, characterization, modification, and adsorption efficacy, pinpointing elements that influence removal efficiency and practical applications. A methodical search was executed across multiple databases utilizing targeted keyword combinations pertinent to biochar and heavy metal remediation. Studies included in the review provided experimental data or synthesised findings regarding biochar's

 doi:10.20944/preprints202605.1519.v1

efficacy, whereas those concentrating exclusively on organic pollutants or lacking adequate methodological detail were omitted. The review recognises limitations, including publication bias and variability in experimental conditions, while delivering a thorough summary of the pertinent literature and findings regarding biochar's adsorption capabilities.

Against this background, the present review has four specific objectives: (i) to synthesise current knowledge on biochar production methods, feedstock selection, and physicochemical characterization as they relate to heavy metal adsorption performance; (ii) to critically evaluate modification strategies (including chemical functionalization, metal impregnation, and composite formation) and their mechanistic contributions to enhanced removal efficiency and selectivity; (iii) to assess the performance of biochar-based systems across industrial, municipal, and agricultural wastewater applications, with explicit attention to operating conditions, adsorption kinetics, isotherm modelling, and regeneration capability; and (iv) to identify key knowledge gaps, with particular emphasis on long-term stability, environmental risk, hybrid AOP integration, and the transition from laboratory-scale evidence to pilot- and field-scale deployment. The scope of the review is confined to peer-reviewed experimental and review literature reporting biochar performance for inorganic heavy metal contaminants (including Pb, Cd, Cr, Cu, Ni, Zn, and As) in aqueous matrices; studies focused exclusively on organic pollutants or soil amendment without a wastewater treatment component are outside its scope. Quantitative life cycle assessment and techno-economic analysis are acknowledged as important complementary tools but are beyond the boundaries of this narrative synthesis.

1.1. Sources of Heavy Metals in Wastewater

Heavy metals present in wastewater originate from a spectrum of natural and anthropogenic activities, with the latter accounting for the vast majority of current contamination trends. Natural contributions, though comparatively smaller in scale, include geological processes such as soil erosion and weathering, volcanic emissions, and aerosol deposition driven by wind or precipitation events. These mechanisms can release trace amounts of metals like arsenic, chromium, and nickel into surrounding watersheds [11]. While such releases are often diffuse and gradual, their background levels set an important ecological baseline against which anthropogenic pollution can be measured. The escalation of industrial activities has led to far higher point-source concentrations entering aquatic systems. Waste streams from mining operations frequently contain acid mine drainage rich in dissolved metal ions; exposure of mined tailings to oxygen and water accelerates leaching of cadmium (Cd), lead (Pb), zinc (Zn), and copper (Cu) into surrounding effluent channels [12]. Metal plating and electroplating facilities produce rinsing waters laden with chromium, nickel, and sometimes silver compounds due to surface treatment formulations [11]. Tanneries employing chromium salts for leather processing are another substantial source, as their effluents carry hexavalent chromium species known for high toxicity and persistence [14,21]. The manufacture of batteries, particularly lead-acid types, releases Pb-rich particulates into both process wastewater and through fugitive emissions that later enter stormwater [12]. Paint production and pigment applications rely on various metallic oxides; improper handling can lead directly to high loads in plant discharge streams. Fertilizer manufacturing incorporates micronutrients such as zinc or copper intentionally; however, impurities like cadmium are also present in phosphate rock feedstocks, allowing inadvertent Cd introduction into both process water and agricultural run-off after soil application [13]. Urban environments contribute through less direct yet cumulatively important pathways. Road traffic generates metallic particulates from brake pad wear (copper, antimony) and tire wear (zinc), which accumulate on surfaces until mobilized by rain events into stormwater drains [11]. This form of diffuse pollution is closely linked with street run-off patterns in densely built areas. Construction activities may release suspended solids containing adsorbed metals from disturbed soil or demolition debris paints that include Pb-based pigments [14]. Agricultural sources deserve particular attention not only for their own contributions but also for their role as intermediaries

 doi:10.20944/preprints202605.1519.v1

transferring metals from other sectors into new environmental compartments. Irrigation with contaminated water enables direct interaction between crops and metal-laden inputs [13].

Livestock wastewater often contains elevated Pb, Cd, or nickel (Ni) due to low assimilation efficiency in animals fed mineral-supplemented feeds; unabsorbed fractions excreted in manure can leach metals during storage or land application events. Over time this contributes to cumulative enrichment of local soils which then acts as a secondary source via erosion into adjacent rivers or groundwater recharge zones [13,14]. Metallurgical industries, steel production or non-ferrous smelting, release multi-metal effluents containing iron (Fe), manganese (Mn), Pb, Cu, Ni, Zn, among others. High thermal discharges associated with these facilities can alter the solubility equilibrium of some species within receiving streams, potentially increasing bioavailable fractions downstream [12]. Petrochemical refineries also participate indirectly: catalytic cracking units employ metals such as nickel and vanadium within catalysts that degrade over time; catalyst fines entering aqueous waste circuits introduce these elements alongside organic hydrocarbons. Municipal solid waste handling systems produce landfill leachate enriched in heavy metals either from corroded metallic waste or from discarded electronics containing circuit boards soldered with Pb-tin alloys. The mixture is chemically complex, often acidic, which enhances the dissolution of bound metals into a mobile ionic form capable of migrating through underlying soils toward aquifers if unmanaged. It is worth noting that the speciation of each metal upon entering wastewater varies considerably depending on its industrial origin. For example, cadmium may be found as Cd ions in galvanization rinsewaters but as organo-cadmium complexes within petrochemical discharges. Such differences influence mobility, toxicity potential, and choice of remediation methods. Hydrological processes accentuate dispersal: high rainfall seasons wash accumulated dry deposition from atmospheric emissions, emitted during fossil fuel combustion, into open channels. Power generation remains a persistent contributor since coal commonly contains mercury (Hg) that volatilizes upon combustion before recondensing on particulate matter subject to wet deposition events [11]. This intricate mosaic of pathways shows that while some contamination routes are tightly coupled to identifiable facilities where pre-treatment could mitigate release volumes, others follow diffuse mechanisms harder to regulate purely at source. Both localized hotspots near industrial zones and broader regional gradients shaped by atmospheric transport emerge when spatially mapping heavy metal burdens across watersheds [13]. Given such diversity in origins, from targeted metallurgical processes to incidental leaks embedded within consumer product life cycles, a one-size-fits-all removal strategy for wastewater treatment remains illusory. Tailored approaches leveraging context-specific contaminant profiles offer better alignment with practical remediation outcomes.

1.2. Impact of Heavy Metals on Environment and Health

Exposure to heavy metals in aquatic systems is a matter of urgent environmental and public health scrutiny, owing to their persistence, toxicity, and ability to bioaccumulate. Even at very low concentrations, elements such as mercury (Hg), chromium (Cr), arsenic (As), cadmium (Cd), and lead (Pb) can exert harmful physiological effects on organisms [14]. The non-biodegradable nature of these metals means they can remain in ecosystems for extended periods, repeatedly cycling through environmental compartments. Once introduced into waterways from industrial effluents or urban runoff, they may settle in sediments where anaerobic conditions can cause remobilization during disturbances such as dredging or flooding. Health consequences in humans vary depending on the exposure route, chemical speciation, and duration. Lead has been linked to severe disorders affecting the nervous system, cognitive development in children, reproductive health, and brain function [15]. Chronic ingestion of lead-contaminated water impairs neurological signaling by disrupting synapse formation and neurotransmitter release. Mercury, particularly in its organic methylmercury form, is notorious for crossing biological membranes and accumulating in neural tissue, leading to cognitive impairment, sensory deficits like deafness and blindness, and systemic effects impacting cardiovascular and immune systems. Extended exposure can manifest clinically as Minamata disease, with profound neurological degeneration. Arsenic contamination produces a spectrum of

 doi:10.20944/preprints202605.1519.v1

symptoms from gastrointestinal distress to carcinogenic effects; prolonged intake can damage skin integrity and compromise multi-organ functionality [16]. Cadmium exposure targets the kidneys and skeletal system. Its tendency to substitute for calcium leads to brittle bone structures over time, while renal accumulation disrupts filtration capacity via proximal tubule damage [17]. Within cellular environments, divalent cations such as Cd trigger oxidative stress responses by generating reactive oxygen species (ROS). These ROS induce DNA damage detectable through genomic assays like microarray profiling [18]. Chromium's toxicity is dependent on valence state; hexavalent chromium [Cr^{6+}], common in tanning wastewaters, acts as a potent oxidizing agent capable of penetrating cell membranes before undergoing intracellular reduction that releases damaging intermediates. The ecological effects mirror many human toxicological pathways but occur across complex food webs. Aquatic organisms accumulate metals through direct exposure or dietary transfer from contaminated prey. Biomagnification causes concentration increases with each trophic level; a small plankton ingests metal-laden particulates; it is consumed by filter feeders; predators higher up take in even greater quantities. Persistent accumulation affects reproductive cycles, growth rates, and survival probabilities. For instance, nickel and copper at levels derived from sludge dumping alter gill morphology in fish, impairing oxygen exchange efficiency [19].

Adsorption onto sediment particles does not equate to permanent removal from biological availability; benthic feeders disturb sediments during feeding activities, reintroducing bound metals into the water column. Secondary environmental impacts arise when elevated heavy metal concentrations select microbial communities carrying metal-resistance genes. Such adaptations can spread horizontally among bacterial populations via mobile genetic elements [14], potentially complicating wastewater treatment processes reliant on microbial metabolism. The emergence of these resistant strains undermines bioremediation techniques otherwise effective against organic pollutants. Heavy metals also engage with other contaminants synergistically or antagonistically in combined pollution scenarios involving dyes or pesticides, as complexation reactions may alter metal solubility or toxicity profiles [20]. Certain dye molecules bind metal ions strongly enough that conventional precipitation fails to remove them entirely. Conversely, some pesticides enhance metal mobility by preventing adsorption onto soil minerals. From an environmental chemistry perspective, speciation controls behaviour within ecosystems. Metals existing predominantly as free ions are highly bioavailable and toxic; conversely, those bound into stable mineral lattices pose less immediate hazard until destabilized by pH shifts or redox changes. For example, acidic mine drainage lowers local pH sufficiently to dissolve insoluble metallic phases into mobile ionic forms that infiltrate downstream groundwater resources [11]. The interplay between contamination intensity and ecological resilience is nuanced. While certain hardy species may withstand higher contaminant loads, thus appearing unaffected, this tolerance often comes at an energetic cost that reduces overall productivity or reproductive success over generations. Sensitive species either decline sharply or relocate if viable habitats remain accessible; these shifts destabilize community composition through loss of keystone organisms that maintain ecosystem balance. Terrestrial implications emerge when irrigation with contaminated water transfers heavy metals into agricultural soils [21]. There they bind variably to organic matter or clay minerals but remain available for uptake into plant tissues under specific conditions like low pH or high salt concentrations. Cereal crops cultivated under such conditions risk passing contaminants directly into human food supplies without any visible signs of distress in plants themselves. At the societal level, chronic exposure scenarios are often compounded by socioeconomic factors limiting access to clean water sources or adequate treatment infrastructure. Populations relying on fishing from contaminated waters face heightened health risks due not just to direct ingestion of water but through dietary accumulation via aquatic protein sources rich in bioaccumulated metals [16]. The hidden nature of sub-lethal effects, neurological impairment without immediate mortality, can delay public recognition until widespread harm has already occurred. In summary of the interconnected damages outlined here, heavy metals represent a dual threat: acute toxicity impacting immediate survival of exposed organisms and chronic degradation eroding long-term ecological stability alongside human health vitality. The difficulty lies in their

 doi:10.20944/preprints202605.1519.v1

persistence across temporal scales far exceeding many remediation timelines [22], meaning interventions must address both active contamination zones and latent reservoirs capable of future release under changing environmental conditions.

2. Production and Characterization of Biochar

2.1. Production Methods for Biochar

Recent advances in biochar characterization and modification methods provide important context for the synthesis and performance data reviewed in this work. Petrović et al., [23] demonstrated that Fe/Mg co-precipitation followed by low-temperature pyrolysis of grape-pomace hydrochar yields a FeMg-modified pyro-hydrochar with maximum Pb^{2+} adsorption capacity of 157.24 mg/g (Sips isotherm; pseudo-second-order kinetics), with FTIR and SEM-EDS evidence confirming chemisorption and ion-exchange as the dominant mechanisms – a modification strategy directly analogous to the composite biochars discussed in Section 2.2. Ercegović et al. [24] further showed that one-step KOH activation of Miscanthus × giganteus at 1073 K produces a hierarchical microporous activated carbon (SSA = 1290 m^2/g) with entropy-driven, spontaneous methylene blue adsorption (qmax up to 463.8 mg/g at 318 K), illustrating how activation conditions govern both pore architecture and thermodynamic adsorption behaviour. At the systems level, Beljin et al. [25] synthesized current knowledge on agricultural waste-derived biochars across water–soil–sediment continua, identifying feedstock variability, pyrolysis temperature, and surface functional group density as the principal determinants of multi-medium remediation performance – considerations that directly inform the characterization framework adopted in Section 2.

In this review, the term 'biochar' is used strictly to denote the carbon-rich solid produced by pyrolysis of biomass under oxygen-limited or anoxic conditions, consistent with the definition adopted by the International Biochar Initiative [26]. Materials produced by hydrothermal carbonization (HTC) are referred to as 'hydrochar', and char recovered as a by-product of gasification is distinguished as 'gasification char'; where findings from these related carbonaceous adsorbents are cited for comparative purposes, the production route is stated explicitly. The principal thermochemical conversion routes – including pyrolysis (the predominant pathway for biochar production), hydrothermal carbonization (yielding hydrochar), and gasification (yielding gasification char) – are illustrated in Figure 1. Each route produces a distinct carbonaceous material whose surface area, porosity, and functional group composition are governed by the specific process conditions applied. The production of biochar begins with the choice of biomass feedstock, a factor exerting substantial influence over the physicochemical characteristics of the final product. Possible inputs include agricultural waste like crop straws, husks, and shells, as well as forestry waste, wood chips, and other organic waste streams [8]. Among these, sugarcane bagasse – an abundant agro-industrial residue generated during sugar extraction – has emerged as a particularly promising feedstock for biochar production. Owing to its high lignocellulosic carbon content and widespread availability, sugarcane bagasse-derived biochar and activated carbon have demonstrated effective removal of heavy metals from aqueous systems, including cadmium and lead, with adsorption capacities comparable to those of commercial activated carbon [27]. This underscores the versatility of agricultural residues as feedstock candidates. Complementing this, Nazbakhsh et al. [28] employed KOH activation with D-optimal design optimization to produce highly porous sugarcane bagasse-derived activated biochar with an exceptional BET surface area of 1149 m^2/g and total pore volume of 0.53 cm^3/g, demonstrating suitability for heavy metal and organic pollutant removal from water. Together, these studies highlight the versatility and potential of sugar industry by-products as low-cost, sustainable precursors for high-performance adsorbents in industrial wastewater treatment. The availability, cost, intrinsic energy content, and desired end-use properties determine the suitability of any given biomass source. Selecting feedstocks with specific mineral compositions or functional group precursors allows scientists to shape biochar's adsorption performance against certain heavy metals by modifying its elemental and surface chemistry during processing. These

 doi:10.20944/preprints202605.1519.v1

differences in the composition of precursor materials result mineral content and porosity. Thermochemical conversion is the foundation of most production methods. Pyrolysis stands as the predominant approach [5]; [4], conducted under oxygen-limited conditions to prevent full combustion while promoting carbonization.

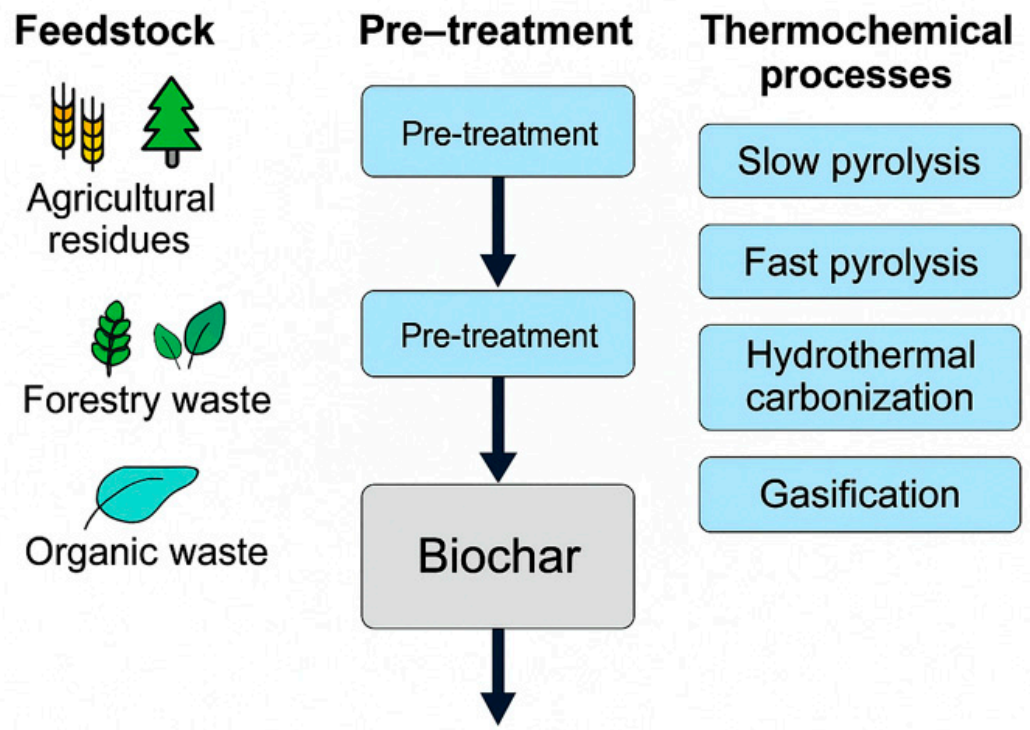

Figure 1. Thermochemical conversion pathways for biomass-derived carbonaceous adsorbents include slow pyrolysis, fast pyrolysis, microwave-assisted pyrolysis (producing biochar), hydrothermal carbonization (yielding hydrochar), and gasification (resulting in gasification char). This review defines 'biochar' as material derived from pyrolysis. Each conversion method results in products with unique physicochemical properties, such as surface area, porosity, aromaticity, and functional group distribution, influenced by factors like feedstock composition, temperature, heating rate, and residence time.

Operational variables, temperature, heating rate, residence time, and atmosphere, act in concert to control pore development, surface area creation, and retention of functional groups [26]. Slow pyrolysis is characterised by low heating rates (typically 1–10 °C min^{-1}), extended residence times of the solid phase (minutes to hours), and reactor temperatures generally in the range of 300–700 °C; these conditions favour carbon retention in the solid phase, yielding the highest biochar mass fractions (25–40% of dry feedstock). Fast (or flash) pyrolysis operates at high heating rates (>100 °C min^{-1}) with very short vapour residence times (0.5–2 s) and peak temperatures of 450–600 °C; the primary product is bio-oil (60–75%), with biochar representing only 10–25% of the yield. An intermediate category (sometimes termed medium or intermediate pyrolysis) employs moderate heating rates and residence times between those of slow and fast pyrolysis, producing roughly equal proportions of bio-oil, biochar, and syngas. It should be noted that temperature ranges across these three modes overlap substantially; it is the combination of heating rate, vapour residence time, and solid residence time, rather than temperature alone, that governs product distribution and the physicochemical properties of the resulting biochar. [1,5]. Higher temperatures tend to increase aromaticity and stability but may diminish oxygenated surface groups important for binding polar contaminants. Alternative thermochemical processes expand beyond traditional pyrolysis. Gasification involves partial oxidation at high temperature where syngas generation is primary; the solid residue (gasification char) is recovered as a secondary product and differs structurally from

 doi:10.20944/preprints202605.1519.v1

pyrolysis-derived biochar due to its higher degree of characterization and lower surface functionality. [29]. Hydrothermal carbonization (HTC) treats biomass in subcritical water environments under elevated pressure. HTC produces hydrochar – a distinct carbonaceous material that differs from pyrolysis-derived biochar in its lower degree of aromaticity, higher oxygen content, and retention of more labile surface functional groups. While hydrochar is not biochar in the strict sense, it shares relevant adsorption properties for heavy metal removal and is included in the comparative discussion where explicitly noted. The oxygen-rich functional groups preserved in hydrochar are useful for metal adsorption [4]. Torrefaction functions at lower temperature ranges (200–300 °C), often as a pre-treatment for biomass intended for subsequent pyrolysis or combustion. Microwave-assisted treatments have been incorporated into magnetic biochar production schemes wherein biochar undergoes post-pyrolysis microwave heating in inert atmospheres after acid treatment [30].

This approach not only modifies pore structure but also facilitates uniform heating that can transform magnetic phases such as FeO into FeO while maintaining active carboxyl sites for enhanced heavy metal sorption capacity. Magnetic biochars offer operational benefits where post-treatment separation from wastewater becomes challenging; external magnetic fields permit rapid recovery from treated water. Feedstock preparation prior to thermal treatment further shapes productivity outcomes. Particle size reduction through grinding or ball milling encourages homogeneous heating during pyrolysis; moisture content must be managed since excess water can prolong drying phases during early thermal escalation and alter chemical yields. Impregnation techniques introduce transitional metals (e.g., iron salts) into biomass prior to pyrolysis; the impregnation-pyrolysis pathway promotes in-situ formation of magnetic phases within the carbonised matrix.[5]. Co-precipitation post-characterization represents another means of embedding metallic species onto biochar surfaces without compromising core structural parameters. Physical activation remains an accessible modification stage post-production. Steam activation develops additional microporosity by etching carbon surfaces and expanding internal pore networks; CO activation operates similarly, though it typically leads to higher surface areas due to slower reaction rates which control burn-off precision.[32]. Air oxidation can introduce new oxygen-containing functionalities beneficial for cationic contaminant attachment without extensive mineral phase modifications. Operational cost assessment intertwines deeply with method selection [5].

While slow pyrolysis is relatively low-tech and yields stable adsorbents suitable for field deployment, methods such as microwave-assisted or magnetic-component additions incur higher energy costs but deliver specialized functionality. Thus, context-specific decision-making is key: removing dispersed heavy metals from mine waste effluents might justify investing in magnetic separation capabilities; conversely, agricultural runoff management may prioritise cost-efficient bulk production from plant residues. Activating environmental sustainability requires balancing resource utilization against contaminant-target removal efficacy. The wide range of available feedstocks means that strategies need to be tailored to each region. For example, forestry residues that are common in some areas may require process optimization that is different from husk-rich outputs that are common near rice-growing areas. Scaling up processes demands predictable property control despite such variability; an engineering challenge linked directly to detailed characterization of both feedstock chemistry and thermal conversion behaviour. Finally, composite material creation blends physical or chemical modifications with base biochar production workflows. [4,5].

This may involve integrating nanoparticles like ZnO or CuO into char surfaces to exploit combined adsorption-precipitation mechanisms for multi-metal solutions. [30]. Such hybrid products build upon conventional thermochemical steps while extending chemical surface repertoire, a reflection of ongoing innovation aimed at meeting increasingly complex wastewater profiles where co-existing contaminants demand multi-modal removal pathways. By integrating flexible feedstock choices with diverse thermal regimes, from slow pyrolysis through advanced microwave treatments, and coupling these with physical or chemical activations, researchers assemble a toolkit capable of tuning biochar properties with considerable precision across target application spectra.[8]. The production methods, feedstock types, and processing conditions employed in biochar synthesis

 doi:10.20944/preprints202605.1519.v1

significantly influence the physicochemical properties and adsorption performance of the resulting material (Table 1).

Table 1. Production of Biochar.

Raw materials	Biochar	Metal Adsorbate	Type of Pyrolysis	Temperature of Pyrolysis	Activation Agent	Ref.
Pinewood	Pine wood biochar	Cr^{6+}, As^{5+}	Slow pyrolysis	300–700 °C	KOH, H_3PO_4	[33]
Orange peel	Orange-peel biochar	Cd^{2+}	Slow pyrolysis	400–800 °C	None	[34]
Orange peel	Citrus peel biochar	Cd^{2+}, Pb^{2+}, Cu^{2+}, organics	Slow pyrolysis	250–500 °C	None, H_3PO_4	[35]
Rice husk	Rice husk biochar	Pb^{2+}, Cd^{2+}, Cu^{2+}	Slow pyrolysis	400–600 °C	None (pristine)	[36]
Rice husk	Activated rice husk biochar	Cd^{2+}	Slow pyrolysis	300–500 °C	KOH	[37]
Coniferous wood	Wood biochar	Cr^{6+}	Standard pyrolysis	Not reported	None	[38]
Poultry litter	Poultry-litter biochar	Cr^{6+}	Pyrolysis	300 °C / 600 °C	None	[39]
Corn stover	Corn stover biochar	Cd^{2+}, Pb^{2+}	Slow pyrolysis	300–600 °C	Steam activation	[40]
Corn straw / Cow dung	Solar-pyrolyzed biochar	Cu^{2+}	Solar pyrolysis	Not reported	None	[40]
Municipal solid waste	MSW biochar	Zn^{2+}, Cu^{2+}, Ni^{2+}	Slow pyrolysis	300–500 °C	H_2SO_4, HNO_3	[42]
Sewage sludge	Sludge biochar	Phosphate, Pb^{2+}, Cd^{2+}, Cu^{2+}, Zn^{2+}	Slow pyrolysis	300–700 °C	MgO, $FeCl_3$	[43,44]

2.1.1. Biochar Modification for Enhanced Metal Removal

Modification of biochar offers a powerful means to amplify its adsorption abilities beyond what is attainable with pristine materials. While unaltered biochars possess inherent porosity and reactive surface groups, these attributes can be selectively adjusted through physical, chemical, and composite-forming strategies to better align with targeted removal needs for heavy metals in complex wastewater matrices. Physical modifications often hinge on altering pore architecture, steam activation or CO_2 activation create new micropores and enlarge mesopores by etching carbon surfaces, expanding accessible internal volume and increasing collision probability between sorbate ions and active sites [45]. Such adjustments directly enhance adsorption kinetics and capacity when dealing with metals that depend heavily on diffusion into fine pore networks. Particle size reduction through milling similarly improves contact efficiency by shortening diffusion pathways. Chemical modification introduces or enriches specific functional groups known for strong affinities toward heavy metal species. Acid treatments, using agents such as HNO_3 or H_2SO_4, can both cleanse ash residues and add oxygenated moieties like -COOH or -OH to the surface (Figure 2) [4].

 doi:10.20944/preprints202605.1519.v1

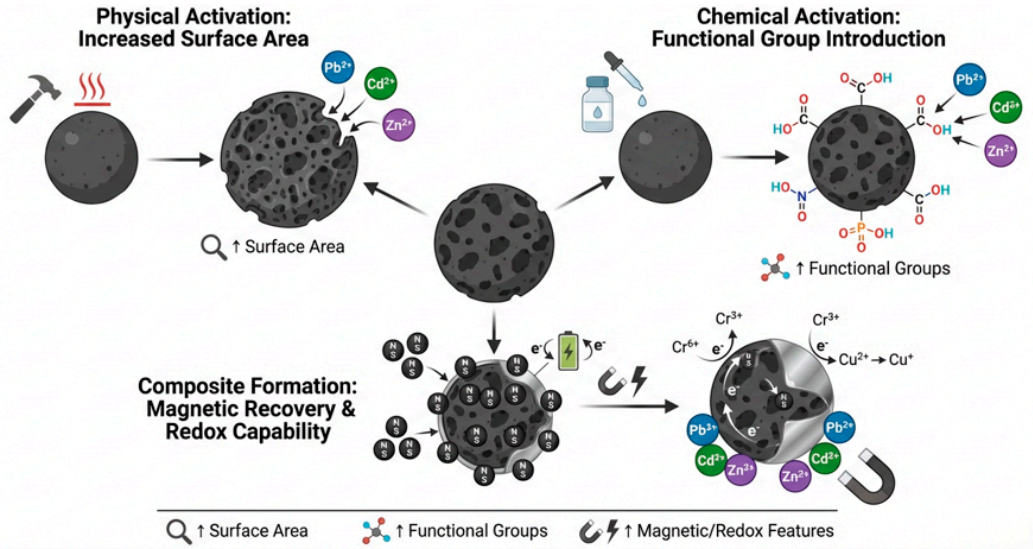

Figure 2. Modification strategies for biochar to enhance heavy metal adsorption, illustrating physical activation (surface area increase), chemical activation (functional group introduction), and composite formation (magnetic recovery and redox capability).

This enrichment bolsters cation exchange capacity and augments complexation potential, especially under pH conditions favoring deprotonation of these groups. Conversely, alkali treatments (e.g., KOH activation) tend to increase surface area and modify surface energetics by generating micropores while also creating negatively charged sites that attract divalent or trivalent cations. Oxidizing agents such as HO have been shown to introduce additional oxygen functionalities that elevate sorption rates due to enhanced hydrophilicity and polar attraction [11]. Organic impregnation takes modification further by grafting molecules onto biochar surfaces that present multi-functional binding sites. Chitosan, a polysaccharide containing hydroxyl (-OH) and amino (-NH) groups, has demonstrated remarkable efficacy when bonded to biochar; it provides both coordination points and hydrogen bonding capabilities conductive to capturing a variety of heavy [5]. Biochars modified in this way outperform their pristine equivalents by orders of magnitude in adsorption capacity for certain cations. Similarly, thiol-functionalized variants prepared via ball milling with 3-mercaptopropyltrimethoxysilane introduce sulphur-based soft donor atoms that bind preferentially to soft acid metals like Hg. Composite formulations expand these concepts through integration with other materials such as clays or metal oxides. Clay-biochar composites can deliver layered adsorption environments where ion exchange within interlayers complements surface complexation mechanisms. [4]. Incorporating iron oxides (FeO, FeOOH) lends magnetic properties useful for post-treatment recovery while simultaneously enabling redox transformations; hexavalent chromium, for example, may be reduced to less mobile Cr^{3+} forms before being immobilized on the composite's surface [21]. Metal impregnation prior to pyrolysis facilitates in-situ formation of such oxide phases embedded within carbon matrices, yielding stable hybrid sorbents that merge multiple removal mechanisms. Adaptations in surface chemistry also influenced mechanistic diversity by boosting ion exchange site density; chemical modifications ensure more predictable binding equilibria even under competitive multi-ion scenarios common in industrial waste streams. For example, nitrogen doping from melamine treatment creates electron-rich domains fostering selective capture via coordinate covalent bonds with transition metals [5]. These changes can shift adsorption behaviour from predominantly physical trapping toward stronger, more irreversible chemisorption interactions. Modification can target structural resilience as well. Low-temperature plasma treatments alter the outermost layers without compromising overall framework integrity; such processes tailor surface polarity while maintaining bulk porosity [21]. This stability serves reuse cycles effectively, modified biochars tend to withstand regeneration procedures better when their functionalization penetrates deeper than superficial coatings susceptible to leaching. Environmental

 doi:10.20944/preprints202605.1519.v1

parameter responsiveness is another benefit emerging from thoughtful modification strategies. Some grafted organic functionalities display minimal loss of activity across wide pH ranges, ensuring consistent performance despite fluctuating wastewater chemistry. In contrast, unmodified oxygenated sites might collapse electrostatic attractions outside narrow pH windows due to protonation-deprotonation dynamics. A specific example illustrating multi-modal modification effects comes from wood-derived biochars altered via acid-based treatments combined with metal oxide loading. Acid-base steps boost micro- and mesoporosity alongside introduction of carboxyl-rich domains; subsequent FeO deposition offers both magnetic separation capabilities and rapid uptake from solution through combined precipitation–complexation pathways [46].

These hybrids remove mixed contaminants efficiently by sequential capture: metals precipitate onto iron phases while residuals engage organic functional sites deeper within pores. Equally relevant are hydrothermal-derived hydrochars modified post-production by alkali oxidation or organic molecule grafting. Although lower in raw surface area compared to pyrolytic products, their preserved oxygen-rich functionality responds well to further attachment of modifiers like amino silanes, yielding sorbents adept at chelating divalent metal ions even under high ionic strength conditions typical of some industrial effluents [11]. Critically assessing trade-offs is essential since some minor yield loss or increased preparation cost often accompanies aggressive modification schemes. The choice between high-surface-area activation versus niche-functionality grafting depends on contaminant profiles: dilute yet diverse pollutant mixtures may benefit more from varied binding chemistries than sheer capacity; conversely concentrated mono-metal loads might justify maximization of active site numbers through intense pore creation methods alone. Overall, the body of work indicates that enhancements achieved via physical restructuring, chemical functionalization, and composite integration consistently extend biochar's utility beyond its pristine performance envelope [45]. By manipulating porosity distributions in tandem with tailored active-group chemistry, modified biochars meet a broader range of operational demands, from fast throughput scenarios requiring quick sorption kinetics to challenging aqueous chemistries demanding specificity and resilience over repeated use cycles. The physicochemical characteristics of biochar, including pore structure, point of zero charge, functional groups, and specific surface area, determine its effectiveness for heavy metal removal from wastewater (Table 3).

Recent advances in biochar modification have demonstrated the effectiveness of bifunctional surface modifications. Zhou *et al.* [47]. developed a chitosan-EDTA bifunctionally modified magnetic walnut shell biochar (E-CMBC) that achieved exceptional copper (Cu^{2+}) removal performance. This three-step synthesis process involved magnetic modification with Fe_3O_4 nanoparticles, surface coating with chitosan, and EDTA grafting via amide bond coupling. The bifunctional modification strategy leverages complementary advantages: walnut shell biochar provides an eco-friendly, low-cost substrate with large surface area and porosity; Fe_3O_4 nanoparticles enable rapid magnetic separation; chitosan provides abundant functional groups (–NH_2/–OH) to enhance Cu^{2+} complexation; and EDTA acts as a strong chelating ligand to improve selectivity and binding affinity. This bifunctional modification approach fills gaps in existing literature by integrating the combined advantages of EDTA (high selectivity), chitosan (abundant complexation sites), and magnetic biochar (easy separation), providing an efficient, sustainable, and engineering-applicable solution for heavy metal pollution control and high-value utilization of agricultural waste.

The material demonstrated a maximum adsorption capacity of 130.8 mg/g for Cu^{2+}, representing a 2.66-fold improvement compared to unmodified magnetic biochar, with 52.4% of equilibrium capacity achieved within 15 minutes [47]. The adsorption mechanism was confirmed to be dominated by dual-functional coordination between carboxyl groups of EDTA and amino groups of chitosan, leading to chemisorption. Kinetic studies showed the process conforms to the pseudo-second-order model, while isotherm analysis fit the Langmuir model ($R^2 = 0.896$), confirming monolayer chemical adsorption at specific binding sites. Thermodynamic analysis revealed the process is spontaneous and endothermic ($\Delta H = 20.94$ kJ/mol, $\Delta S = 106.5$ J/mol·K), with entropy increase serving as the primary driving force. The material maintained high adsorption efficiency across pH 3-5, exhibited

 doi:10.20944/preprints202605.1519.v1

strong selectivity against coexisting ions (Na^+, K^+, Ca^{2+}, Mg^{2+}), and enabled rapid magnetic separation within seconds under an external magnetic field [47]. Competitive adsorption studies revealed that E-CMBC exhibits "valence state dependence" in its selectivity: extremely strong selectivity for monovalent Na^+ and K^+ (selectivity coefficient $K > 20$ even under 10-fold concentration interference), while showing more moderate selectivity for divalent Ca^{2+} and Mg^{2+} (K = 1.86-2.33 under 10-fold interference). This selectivity stems from the synergistic effect of EDTA chelation specificity, chitosan coordination preference, and bifunctional layer spatial screening. The six-tooth chelating structure of EDTA is highly compatible with Cu^{2+} ion configuration, forming stable chelating rings with minimal tension, while its structural specificity makes binding priority for Cu^{2+} much higher than for other ions [47]. For regeneration and reusability, E-CMBC demonstrated excellent performance with 0.1 M Na_2EDTA solution as the desorption agent. After five consecutive adsorption-desorption cycles, the material retained 91.13% of its initial adsorption capacity. The EDTA modification appears to have stabilized the adsorbent, enhancing its resilience in acidic conditions and making it suitable for repeated use in practical wastewater treatment applications [47].

2.2. Physicochemical Characteristics of Biochar

The physicochemical characteristics of biochar largely dictate its suitability for heavy metal remediation in wastewater systems. Its performance emerges from an interplay between morphological features, chemical functionalities, and inherent mineral compositions shaped by feedstock choice and processing conditions. One of the most defining physical traits is the hierarchical pore structure comprising micropores (< 2 nm), mesopores (2–50 nm), and macropores (> 50 nm). Each pore category contributes differently: micropores act as confined trapping sites favoring adsorption via size exclusion or van der Waals forces; mesopores function as conduits for mass transfer, allowing contaminants to diffuse into interior regions; macropores facilitate bulk fluid flow and enhance contact between sorbate molecules and the internal adsorption surfaces [32]. The specific surface area, a central factor for adsorption capacity, is sensitive to pyrolysis temperature. Elevated temperatures generally increase surface area and microporosity while boosting hydrophobicity, augmenting affinity for less polar substrates. Conversely, lower-temperature biochar's often preserve abundant oxygen-containing functional groups that promote electrostatic attraction and complexation with polar species such as metal cations [5]. The presence of these functionalities, carboxyl (-COOH), hydroxyl (-OH), carbonyl (C=O), directly influences cation exchange capacity and facilitates multiple mechanisms including ion exchange, surface precipitation, and chelation [48]. Morphological variation extends beyond porosity. Surface roughness impacts how readily aqueous contaminants anchor to adsorption sites. Modification techniques, including acid-base treatments, steam activation, impregnation with metal oxides or salts, can alter both external morphology and internal pore distribution.

2.2.1. Surface Characterization

BET Surface Area:

The Brunauer-Emmett-Teller (BET) equation calculates specific surface area [42]:

$$\frac{1}{W\left[\left(\frac{P_0}{P}\right)-1\right]} = \frac{C-1}{W_m C} \times \frac{P}{P_0} + \frac{1}{W_m C} \quad \text{(Eq. 1)}$$

where W = weight of gas adsorbed at relative pressure P/P_0; W_m = weight of adsorbate as monolayer; C = BET constant; P/P_0 = relative pressure.

Surface area (S_{BET}) is calculated as [43]:

$$S_{BET} = \frac{W_m N_A \sigma}{M} \quad \text{(Eq. 2)}$$

where N_A is Avogadro's number (6.022×10^{23} molecules/mol), σ is the cross-sectional area of adsorbate molecule (Å^2), and M is molecular weight of adsorbate.

 doi:10.20944/preprints202605.1519.v1

Simplified Estimation for Routine Analysis

For nitrogen adsorption at 77 K (the most common BET measurement condition), a simplified relationship exists [44]:

where V_m = monolayer volume in mL/g (STP); 4.35 = conversion factor for N_2 at 77 K

Total Pore Volume

$$V_{pore} = \frac{V_{ads} \times 0.001547}{\rho_{liquid}} \quad \text{(Eq. 3)}$$

where Vads is the adsorbed gas volume at standard conditions (cm^3/g STP) and ρ liquid is the density of liquefied adsorbate [45].

Point of Zero Charge (pHpzc)

Determined experimentally by plotting ΔpH versus initial pH:

$$\Delta pH = pH_{final} - pH_{initial} \quad \text{(Eq. 4)}$$

At pHpzc: ΔpH = 0

Acid treatments might increase microporosity by etching carbon matrices but can also introduce negatively charged functional groups enhancing selectivity for positively charged ions. Alkali activation frequently expands total pore volume while improving surface area values relative to pristine biochar [53], potentially offering greater accessibility for bulky polyvalent ions. Chemical composition is another determinant; inherited mineral fractions from the feedstock, carbonates, phosphates, silicates, contribute adsorption pathways beyond pure surface bonding. Calcium-rich matrices may drive precipitation reactions with dissolved Pb or Cd ions through insoluble carbonate phase formation [54] Silica phases common in rice husk-derived biochar can facilitate structural stability while interacting with certain transition metals via surface silanol groups. Such mineral-assisted adsorption complements direct organic functional group interactions. pH sensitivity remains a notable chemical characteristic affecting performance outcomes. At lower pH values, protonation of oxygen sites reduces negative charge density on the biochar surface, diminishing electrostatic attraction toward cations. Under alkaline conditions, deprotonation enhances negative charges which can strengthen binding affinity for divalent and trivalent metal ions; however excessive alkalinity may induce competing precipitation phenomena within bulk solutions rather than in pores themselves. This competition between solution-phase precipitation and sorbent-surface fixation must be considered when interpreting adsorption data under varying environmental chemistries. Biochar's electrical properties also influence adsorptive behaviour. Surface charge distribution depends on both feedstock ash content and processing regime. Higher ash content typically raises pH (point of zero charge), modifying interaction potential with contaminants exhibiting certain ionic states at given environmental pH values [55].

Electrostatic forces work alongside weaker physico-sorption processes in capturing metallic species from solution; effective removal often results from a combination rather than either mechanism in isolation. Moisture content during storage or application influences physicochemical stability by modulating functional group activity through hydration/dehydration cycles. In practical terms, retained water within pores can block access to active sites or alternatively aid contaminant diffusion depending on solute polarity and ionic strength in the surrounding medium [56].

Biochars rich in hydrophilic groups tend to hold more bound water which could facilitate hydration shell-mediated ion transport into inner structures before ultimate fixation at active sites. Composite forms offer a route to expand process-specific performance by integrating materials such as clays or metal oxides into the carbon matrix [57]. Clay-modified variants often extend accessible surface area while providing layered structures that intercalate organic pollutants alongside metals. Metal oxide-loaded biochars exploit redox capabilities for transforming toxic metal species into less mobile forms in situ, FeO additions may catalyze oxidation-reduction reactions altering Cr^{6+} to Cr^{3+} which binds more strongly to carboxylated surfaces. These synergies depend upon intimate contact

 doi:10.20944/preprints202605.1519.v1

between composite phases at nano- to microscale levels inside biochar's complex network of pores and fractures. Production conditions strongly imprint physicochemical signatures relevant to field applications discussed earlier. For example, hydrothermal carbonization yields hydrochars with inherently lower surface areas than pyrolytic counterparts due to extensive retention of oxygen functionality within less graphitized structures [11], which may suit removal of inorganic polar contaminants rather than nonpolar organics where higher hydrophobicity would be favored. Gasification-derived chars often hold distinct mineral textures owing to partial oxidation atmospheres altering ash chemistry, these differences manifest noticeably when comparing adsorption isotherms across production methods using identical feedstocks. Finally, variability introduced through biomass heterogeneity makes standardization a challenge yet offers an advantage in tuning outcome profiles for specific wastewater types. Fine control of the balance between micro/mesoporosity and reactive functional group density appears essential for designing efficient biochars adapted to treatment objectives, whether maximizing uptake rates under high-flow scenarios or focusing on tight binding where low contaminant concentrations necessitate durable retention over extended residence times [46].

The adsorption behaviour of heavy metals on the surfaces of biochar depends on the pore structure, the point of zero potential, specific surface area and functional groups as shown in Table 2. Figure 3 illustrates the influence of pyrolysis temperature on the key physicochemical properties of biochar, including specific surface area, pore size distribution, functional group density, and ash content. As shown, increasing the pyrolysis temperature promotes the development of micropores and enhances surface area, while simultaneously reducing oxygen-containing functional groups. These temperature-dependent shifts directly affect biochar's adsorption performance and help explain the variability reported across different studies.

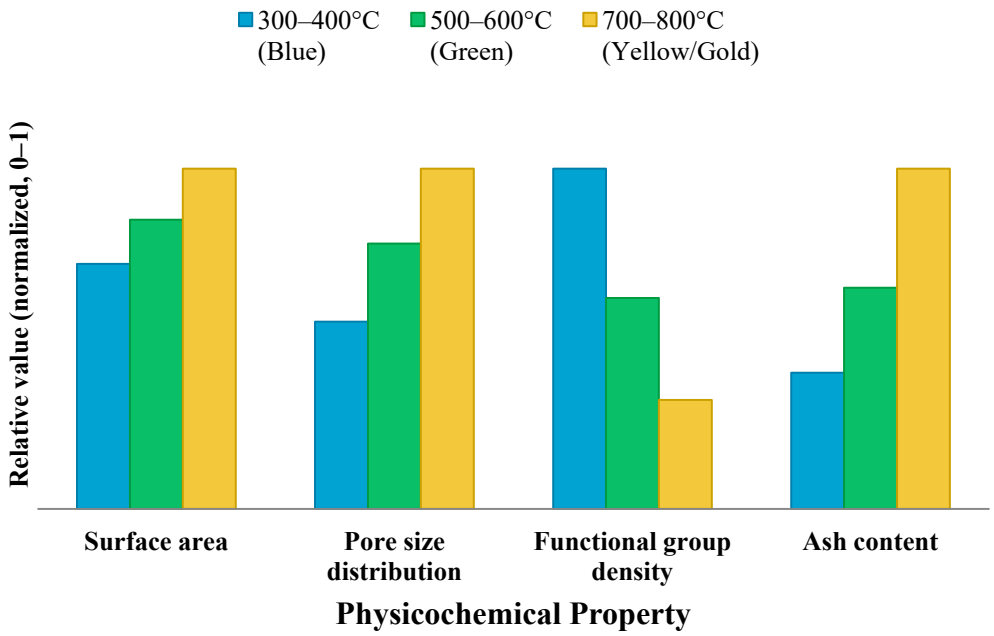

Figure 3. Effect of Pyrolysis Temperature on Biochar Physicochemical Properties.

Table 2. Characteristics of Biochar.

Biochar	Metal adsorbate	Pore Structure	Point of Zero Charge (pHpzc) [pH drift method	Functional Groups	Specific Surface Area (m^2/g) [BET-N_2, 77	Ref

 doi:10.20944/preprints202605.1519.v1

			where reported]		K where reported]	
Chicken manure biochar (CM400, 400°C)	Pb^{2+}	Mesopores (2-50 nm), avg. pore diameter 4.69-9.12 nm	~8.0	-OH, aliphatic CH_2, C=O (carboxyl), C=C, C-O, Si-O-Si	44.87	[121]
Bamboo biochar (BB600, 600°C)	Pb^{2+}	Mesopores, total pore volume 524.17 mm^3/g	NR	-OH, C=O, C=C (aromatic), CO_3^{2-}, PO_4^{3-}	447.46	[58]
Peanut hull biochar (450°C)	Pb^{2+}, Cd^{2+}	Porous structure	NR	--OH, C=C, C=O (aromatic), CO_3^{2-}, PO_4^{3-}, Si-O-Fe	NR	[59]
Pinewood biochar (PC, 700°C)	Pb^{2+}, Cd^{2+}	Well-developed micropores and mesopores	NR	-OH, CH_2, C=C, C-O, C-O-C	320.5 (UV-modified: 522.3)	[60]
Bamboo biochar (BC, 700°C)	Pb^{2+}, Cd^{2+}	Microporous and mesoporous	NR	-OH, C=C (aromatic), C-O	148.6 (UV-modified: 471.1)	[60]
Urban pruning biochar (Lv700-63, 700°C)	Pb^{2+}, Cd^{2+}, Mn^{2+}	Heterogeneous, wide porous, mesopores + micropores	NR	Hydroxyl groups, aromatic C-H, aromatic C=C	29.94	[61]
Empty fruit bunch biochar (F-EFBB, fine)	Pb^{2+}	Exposed inner pores	NR (qualitative: low, net negative surface; numeric value not reported)	-OH, -COOH, C=O (throughout matrix)	NR	[62]
Modified reed biochar (MRBC, with Fe)	Cd^{2+}, Pb^{2+}	NR	NR	-OH, C=O, C-O, FeO_x groups	NR	[63]
SiO_2NPs@BC (silkworm excrement)	Cd^{2+}	Well-developed, pore volume 0.608 cm^3/g	NR	Si-C, Si-O, Si-O-Si	46.58	[64]
Tea waste biochar/ZIF-67 (CMCB@TWBM/ZIF-67)	Pb^{2+}, Cd^{2+}	Hierarchical porous structure	NR	-OH, C-H/CH_2, carboxyl groups	25.7	[65]
Corn stalk biochar - Raw Carbon (RC)	Cr^{6+}	Graphite structure	8.2-9.5 (alkaline)	Hydroxyl, carboxyl, aromatic π-electrons	NR	[66]
Corn stalk biochar - Organic Component (OC)	Cr^{6+}	Graphite structure (enhanced)	6.5-7.5	Enhanced hydroxyl, carboxyl groups	NR	[66]
Activated carbon (AC)	Cd^{2+}, Pb^{2+}	Microporous + mesoporous	10.01 ± 0.03 (	-OH, C=O, C-O, carboxyl groups	1018	[67,68]

 doi:10.20944/preprints202605.1519.v1

Bamboo biochar (BB)	Cd^{2+}, Pb^{2+}	Mesoporous	9.27 ± 0.01	-OH, C=O, C=C, carboxyl	310	[67,68]
Palm shell biochar (PSB)	Cd^{2+}, Pb^{2+}	Less developed porosity	7.69 ± 0.07	-OH, C=O, C-O	125	[67,68]
Mangrove wood biochar (MB)	Cd^{2+}, Pb^{2+}	Moderate porosity	7.58 ± 0.07	-OH, C=O, carboxyl	182	[67,68]
Rhododendron residue biochar (RRB, 600°C)	Heavy metals	3Mesoporous + microporous	NR	-OH, C=O, C=C, carboxyl	412	[69]

Notes: NR = Not Reported in the cited source (the parameter was not measured or disclosed by the original authors; data may be obtainable directly from authors). N/A = Not Applicable (the parameter does not apply to this material or experimental context). pHpzc values were determined by the pH drift method where reported; entries without an explicit method statement are marked NR. Specific surface area values were measured by BET N_2 adsorption at 77 K where reported; entries without confirmed measurement conditions are marked NR. Cross-study comparison of surface area and pHpzc values should account for differences in degassing temperature, relative pressure range, and equilibration protocol.

3. Mechanisms of Heavy Metal Adsorption on Biochar

3.1. Adsorption Processes

Adsorption processes form the primary pathway through which biochar captures and retains heavy metals from aqueous environments. The interplay of surface chemistry, pore architecture, and mineral phases inherent to the biochar structure dictates how these metals are immobilized. Multiple concurrent mechanisms operate during adsorption, making it a synergistic phenomenon rather than the result of a single interaction type. The presence of oxygen-containing functional groups such as hydroxyl (-OH), carboxyl (-COOH), carbonyl (C=O), and phenolic moieties offers coordination sites for cations in solution, enabling complexation reactions that produce stable metal-organic surface complexes [70]. These interactions are often pH-dependent; under alkaline conditions, deprotonation of these groups increases the negative charge density on the biochar surface, strengthening electrostatic attraction towards positively charged metal ions like Pb, Cd, Cu, and Zn [55]. Electrostatic attraction complements complexation by drawing cations toward negatively charged areas on biochar surfaces. This is particularly effective in biochars with high ash content or those derived from feedstocks rich in minerals that confer a net negative surface potential [71].

Ion exchange serves as another critical removal mechanism; metal ions in solution replace naturally occurring cations such as K, Na, Ca or Mg bound to functional groups within the biochar matrix [2].This exchange is facilitated by the porous network that allows close proximity between mobile ions and exchangeable sites. Physical adsorption (physico-sorption) operates alongside chemisorption mechanisms to trap dissolved metals within micro- and mesopores via van der Waals forces and pore confinement effects. The high specific surface area observed in well-activated biochar's maximizes potential contact points, creating numerous loci where weak interactions can hold metals until more permanent fixation occurs through other processes [72]. Pore diffusion further ensures that ions migrate inward toward active centres, large mesopores act as transport channels while micropores become ultimate storage sites. Biochars functionalized with multiple organic groups often display combined physisorption and chemisorption characteristics; porous structure works to concentrate solute near chemically active sites embedded deeper within the matrix [73].

Surface precipitation represents an additional pathway when local chemical conditions favor formation of insoluble mineral phases at or near the biochar interface. For example, carbonate-rich biochars arising from certain plant residues may precipitate Pb or Cd as carbonates directly onto external surfaces or within pores [74]. Co-precipitation also occurs when dissolved metals incorporate into growing mineral structures initiated by existing inorganic phases within the char. Biochar's adsorption performance is strongly influenced by feedstock-derived mineralogy and post-

 doi:10.20944/preprints202605.1519.v1

modifications. Embedding iron compounds, either through pre-treatment impregnation or post-pyrolysis loading, can induce redox transformations where more toxic species are converted into less mobile forms before binding irreversibly. Ferrous sulphide additions have been shown to facilitate reduction of As^{5+} to less toxic As^{3+} simultaneously with adsorption onto Fe-bearing surfaces [75]. In similar fashion, inclusion of manganese oxide groups can enhance multi-metal uptake due to their variable oxidation states accommodating different metal valences [76]. Functional group engineering via chemical treatment drastically alters adsorption pathways. Introducing nitrogen-containing moieties broadens interaction types by permitting hydrogen bonding in addition to classical coordination chemistry between lone pairs on nitrogen atoms and vacant orbitals on metal cations. Thio-amide functionalities target soft acid cations like Hg through sulphur-metal affinity stronger than oxygen bindings [73].

Carboxylic acids remain versatile across many metals because their conjugate base form persists over a wide pH range relevant to wastewater scenarios. Hydrothermal processing results in hydrochars that differ from purely pyrolytic materials yet still leverage oxygen-rich functionality for effective complexation. Although possessing lower surface areas, their abundance of accessible polar sites fosters strong affinity for divalent metal species [11]. Where contaminant profiles include both cationic metals and nonpolar organics, partitioning processes come into play: hydrophobic domains tend to capture organic molecules while hydrophilic regions bind metals. Biochar removes heavy metals from wastewater through several concurrent mechanisms, as illustrated in Figure 4. These include: (i) electrostatic attraction and ion exchange, whereby negatively charged surface functional groups (carboxylates, phenolates) attract and exchange divalent and trivalent metal cations such as Pb^{2+}, Cd^{2+}, and Cu^{2+}; (ii) complexation and chelation, in which carboxyl (–COOH), hydroxyl (–OH), and phenolic (Ph–OH) groups form stable coordinate bonds with metal ions; (iii) reductive transformation, most notably the reduction of toxic hexavalent chromium Cr^{4+} to the less mobile Cr^{3+} via electron donation from biochar's carbon matrix; and (iv) mineral co-precipitation, where dissolved metals form insoluble precipitates such as $Pb_3(PO_4)_2$ and $Fe(OH)_3$ within or on the biochar surface. In practice, these pathways operate simultaneously rather than in isolation, and their relative contributions depend on the metal species, solution pH, ionic strength, and the surface chemistry of the specific biochar. Together, they underpin the broad-spectrum heavy metal removal capability that makes biochar an attractive alternative to conventional adsorbents.

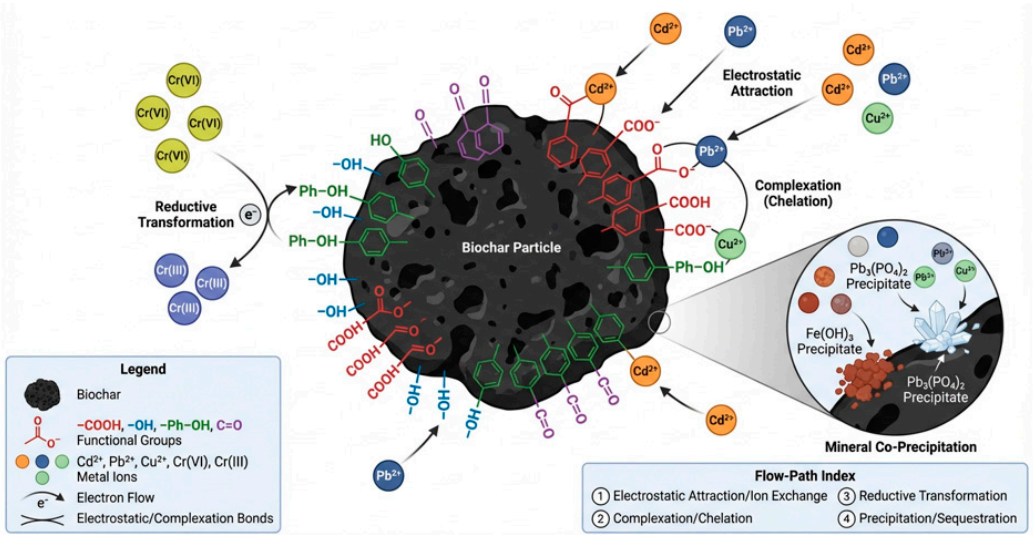

Figure 4. Mechanisms of Biochar–Metal Interactions with Functional Groups and Redox Processes.

This duality benefits multi-contaminant wastewater streams encountered in industrial disposal scenarios. The specificity of adsorption can vary across different metals depending on ionic radius, hydration energy, and affinity for particular functional groups present in a given biochar sample. For

 doi:10.20944/preprints202605.1519.v1

example, smaller hydrated ions like Cu may diffuse rapidly into narrow micropores but could compete unfavorably against larger Pb ions for coordination with carboxyl sites if steric factors dominate binding behaviour [10].`Selective sorption has thus been observed with certain composites where size-exclusion effects combined with tailored chemical affinities produce ordered uptake sequences across mixed-metal solutions. Environmental conditions modulate adsorption efficacy dynamically. Ionic strength impacts double-layer thickness around negatively charged surfaces; higher salt concentrations compress electrical double layers thereby reducing electrostatic attraction range but potentially increasing localized ion clustering conducive to precipitation at interfaces [55]. Similarly, temperature shifts alter kinetic parameters, higher thermal energy accelerates diffusion rates though may weaken weaker physico-sorption forces holding loosely bound species. A noteworthy operational aspect is adsorbent reuse potential following desorption steps conducted under controlled pH swings or use of chelating eluents. Preserving structural integrity during regeneration depends on avoiding chemical treatments that degrade pore networks or strip essential site functionalities introduced during initial modification phases [2]. Developing regeneration protocols that maintain adsorptive capacity remains tied to understanding how each contribution mechanism, from ion exchange through precipitation, affects resilience under repeated use cycles. Ultimately, the adsorption processes woven throughout biochar's interaction with heavy metals represent interconnected pathways governed by molecular-scale attributes of its carbon matrix along with embedded minerals and deliberately engineered functionalities [71]. Recognizing this complexity allows for rational design choices aimed at maximizing removal efficiency under real-world wastewater conditions where multicomponent systems challenge simplistic one-mechanism interventions.

3.2. Mathematical Modelling of Adsorption Processes

Understanding the mechanisms and efficiency of heavy metal removal by biochar requires quantitative analysis through mathematical models. These models describe adsorption equilibrium, kinetics, thermodynamics, and process efficiency, providing essential tools for designing and optimizing biochar-based treatment systems.

Definition of Adsorption Capacity

The fundamental parameters for evaluating biochar performance are adsorption capacity and removal efficiency. Adsorption capacity at equilibrium5(q_e) quantifies the mass of adsorbate per unit mass of adsorbent:

$$q_e = \frac{(C_0 - C_e) \times V}{m} \quad \text{(Eq. 5)}$$

where q_e = adsorption capacity at equilibrium (mg/g); C_0 = initial metal concentration (mg/L); C_e = equilibrium metal concentration (mg/L); V = volume of solution (L); m = mass of biochar (g).

For time-dependent studies, the adsorption capacity at time t (q_t) is calculated as:

$$q_t = \frac{(C_0 - C_t) \times V}{m} \quad \text{(Eq. 6)}$$

where C_t is the metal concentration at time t.

Adsorption Isotherm Models

Isotherm models describe the distribution of adsorbate molecules between liquid and solid phases at equilibrium. The most commonly applied models for biochar systems are Langmuir and Freundlich isotherms [77**]: [78].**

Langmuir Isotherm Model

The Langmuir model assumes monolayer adsorption on a homogeneous surface with finite identical sites and no interaction between adsorbed molecules [78]:

 doi:10.20944/preprints202605.1519.v1

$$q_e = \frac{q_{max} \times K_L \times C_e}{1 + K_L \times C_e} \quad \text{(Eq. 7)}$$

The linearized form facilitates parameter determination:

$$\frac{C_e}{q_e} = \frac{1}{q_{max} \times K_L} + \frac{C_e}{q_{max}} \quad \text{(Eq. 8)}$$

where q_{max} = maximum monolayer adsorption capacity (mg/g); K_L = Langmuir equilibrium constant (L/mg).

A dimensionless separation factor (R_L) indicates adsorption favourability:

$$R_L = \frac{1}{1 + K_L \times C_0} \quad \text{(Eq. 9)}$$

Values of $0 < R_L < 1$ indicate favourable adsorption; $R_L > 1$ suggests unfavourable adsorption; $R_L = 1$ represents linear adsorption; and $R_L = 0$ indicates irreversible adsorption.

Freundlich Isotherm Model

The Freundlich model describes multilayer adsorption on heterogeneous surfaces with non-uniform distribution of adsorption heat [79]:

$$q_e = K_F \times C_e^{1/n} \quad \text{(Eq. 10)}$$

The linearized form:

$$\log\ q_e = \log\ K_F + \frac{1}{n} \log\ C_e \quad \text{(Eq. 11)}$$

where K_F = Freundlich constant related to adsorption capacity [(mg/g)(L/mg)^1/n^]; n = heterogeneity factor.

When $1 < n < 10$, adsorption is favourable; $n < 1$ indicates cooperative adsorption; and $n > 10$ suggests very weak adsorption.

Adsorption Kinetic Models

Kinetic models describe the rate of adsorption and the time required to reach equilibrium, providing insights into adsorption mechanisms and mass transfer processes.

Pseudo-First-Order Model

Based on Lagergren's equation, this model assumes adsorption rate is proportional to the number of unoccupied sites [80]:

$$\frac{dq_t}{dt} = k_1(q_e - q_t) \quad \text{(Eq. 12)}$$

Linearized form:

$$\log\ (q_e - q_t) = \log\ q_e - \frac{k_1}{2.303} t \quad \text{(Eq. 13)}$$

where k_1 is the pseudo-first-order rate constant (min^{-1}).

Pseudo-Second-Order Model

This model assumes chemisorption as the rate-limiting step:

$$\frac{dq_t}{dt} = k_2(q_e - q_t)^2 \quad \text{(Eq. 14)}$$

Linearized form:

$$\frac{t}{q_t} = \frac{1}{k_2 q_e^2} + \frac{t}{q_e} \quad \text{(Eq. 15)}$$

 doi:10.20944/preprints202605.1519.v1

where k_2 is the pseudo-second-order rate constant (g/mg·min).

The initial adsorption rate (h, mg/g·min) is:

$$h = k_2 q_e^2 \quad \text{(Eq. 16)}$$

The isotherm and kinetic models for different metals and biochar are summarized in Table 3, which now includes comparability metadata (initial concentration (C_0), adsorbent dose, pH, temperature, and matrix type) for each study to enable meaningful cross-study evaluation. Because q_{max} values from the Langmuir model are only directly comparable when experimental conditions (C_0, dose, pH, and matrix type) are similar, readers are advised to compare entries within like-for-like subsets. For instance, the Pb^{2+} subset at pH ≈ 5, 25 °C, and synthetic water conditions spans q_{max} values from 7.48 mg/g (palm kernel shell) to 361.2 mg/g (Ca-modified biochar), illustrating how modification strategy rather than differences in experimental protocol drives the observed range. The maximum adsorption capacity (q_{max}) varied with the biomass, the pH optimum for biosorption. The kinetic model commonly observed is the pseudo second order model.

Table 3. Best-Fit Isotherm and Kinetic Models for Biosorption of Heavy Metals on Biochar (with Comparability Metadata).

Biochar Material	Metal	C_0 (mg/L)	Dose (g/L)	pH	T (°C)	Contact Time	Matrix Type	Best-Fit Isotherm	Best-Fit Kinetic	q_{max} (mg/g)	K_L (L/mg)	K_F/n	Ref.
Lead (Pb^{2+})													
Cattle manure biochar (CMB6)	Pb^{2+}	50–200	2	5–6	25	120 min	Synthetic	Langmuir	Pseudo-2nd order	**40.8–51.87**	N/A	N/A	[13]
Sheep manure biochar (SMB3)	Pb^{2+}	5–100	5	5–6	25	60 min	Synthetic	Langmuir-Freundlich	Pseudo-2nd order	**20.2**	N/A	N/A	[82]
Palm kernel shell biochar	Pb^{2+}	10–100	1	5	25	150 min	Synthetic	Langmuir (R^2=0.948)	Pseudo-2nd order	**7.48**	N/A	1.86	[83]
Bagasse biochar	Pb^{2+}	10–200	2	5	25	140 min	Synthetic	Langmuir	Pseudo-2nd order	**12.741**	N/A	N/A	[84]
Pulverized wood-derived biochar (PWB)	Pb^{2+}	10–300	2	5.1	25	200–150 min (740°C)	Synthetic	Langmuir	Pseudo-2nd order	N/A	N/A	N/A	[85]
Ca-modified biochar (BC-Ca-P)	Pb^{2+}	10–400	2	5	25	120 min	Synthetic	Langmuir	Pseudo-2nd order	**361.2**	N/A	N/A	[86]
Pine needle biochar at 550°C (Himalayan)	Pb^{2+}	10–200	2	5	35	24 h (equilibrium)	Synthetic	Langmuir	Pseudo-2nd order	**40.4**	N/A	N/A	[87]
Cadmium (Cd^{2+})													
Cattle manure biochar (CMB6)	Cd^{2+}	50–200	2	5–6	25	120 min	Synthetic	Langmuir	Pseudo-2nd order	**23.08–26.78**	N/A	N/A	[13]
Sheep manure biochar (SMB3)	Cd^{2+}	5–100	5	5–6	25	60 min	Synthetic	Langmuir-Freundlich	Pseudo-2nd order	**3.2**	N/A	N/A	[82]
Coconut shell	Cd^{2+}	10–200	2	5	25	360 min	Synthetic	Langmuir	Pseudo-2nd order	**63.88**	N/A	N/A	[88]

 doi:10.20944/preprints202605.1519.v1

biochar (CS@BC)													
Cassava root husk biochar (CRHB)	Cd^{2+}	10–100	2	6	25	60 min	Synthetic	Langmuir	Pseudo-1st & 2nd order	**26.42**	N/A	N/A	[89]
Euhalophyte-derived biochar (Salicornia europaea) (SBC)	Cd^{2+}	10–80	1	6	25	120 min	Synthetic	Langmuir	Intraparticle diffusion + others	**108.54**	N/A	0.1–0.5	[13]
Wood biochar (Iris sibirica L.)	Cd^{2+}	5–80	4	N/A	25	N/A	Synthetic	Langmuir + Freundlich	Pseudo-2nd order	**19.9**	N/A	N/A	[90]
Copper (Cu^{2+})													
Cattle manure biochar (CMB6)	Cu^{2+}	50–200	2	5–6	25	120 min	Synthetic	Langmuir	Pseudo-2nd order	**13.9–25.1**	N/A	N/A	[13]
Glycine-enriched biochar (GBC)	Cu^{2+}	10–200	1	5–6	25	600 min	Synthetic	Langmuir	Pseudo-2nd order	**N/A**	N/A	N/A	[91]
Optimised biochar (Cu-BC)	Cu^{2+}	10–300	1.5	5.5	25	240 min	Synthetic	Langmuir	Pseudo-2nd order	**210.56**	N/A	N/A	[92]
Nickel (Ni^{2+})													
Cattle manure biochar (CMB6)	Ni^{2+}	50–200	2	5–6	25	120 min	Synthetic	Langmuir	Pseudo-2nd order	**23.18–27.31**	N/A	N/A	[13]
Glycine-enriched biochar (GBC)	Ni^{2+}	10–200	1	5–6	25	600 min	Synthetic	Langmuir	Pseudo-2nd order	**N/A**	N/A	N/A	[91]
Rice straw biochar	Ni^{2+}	5–100	5	5–6	25	180 min	Synthetic	Langmuir	Pseudo-2nd order	**13.348 (mg/kg)**	N/A	N/A	[82]
Coir pith biochar (mesh)	Ni^{2+}	10–100	2	7	25	Equilibrium	Synthetic	Langmuir (R^2=0.992)	Pseudo-2nd order (R^2=0.970)	**99.8**	N/A	N/A	[93]
Sewage-sludge biochar + α-Fe_2O_3	Ni^{2+}	5–200	2	7	25	~60 min	Synthetic	Langmuir	Pseudo-2nd order	**35.5**	N/A	N/A	[94]
Chromium (Cr^{6+} / Cr^{6+} / Cr^{3+})													
Corn stalk biochar	Cr^{6+}	5–100	5	1	25	240 min	Synthetic	Freundlich	Pseudo-2nd order	**435.25**	N/A	N/A	[82]
Chestnut shell biochar (PCNi3)	Cr^{6+}	10–200	1	2	25	1440 min	Synthetic	Langmuir-Freundlich-Sips	Pseudo-2nd order	**171.43**	166.89	N/A	[95]
Rice straw magnetic biochar (BMBC)	Cr^{6+}	10–200	1	2	25	1440 min	Synthetic	Langmuir	Pseudo-2nd order	**66.1**	N/A	N/A	[96]
Rice husk biochar	Cr^{6+}	10–500	1	4	25	270 min	Synthetic	Langmuir	Pseudo-2nd order	**435**	N/A	N/A	[97]

 doi:10.20944/preprints202605.1519.v1

Cassava root husk biochar (CRHB-ZnO)	Cr^{6+}	10–100	2	6	25	60 min	Synthetic	Langmuir	Pseudo-1st & 2nd order	**28.37**	N/A	N/A	[88]
Camel dung biochar	Cr^{3+}	10–150	2	Unspecified	25	N/A	Synthetic	Langmuir + Freundlich	Pseudo-2nd order	**~23.4**	N/A	N/A	[98]
Jacaranda fruit pod biochar (500°C, H_3PO_4-activated)	Cr^{6+}	10–200	1	2	25	180 min	Synthetic	Langmuir	Pseudo-2nd order	**208.3**	N/A	N/A	[99]
Beechwood chip + garden green waste biochar	Cr^{6+}	10–100	2	5	25	Unspecified	Synthetic	Freundlich + Langmuir	Pseudo-2nd order	**N/A**	N/A	N/A	[100]
Zinc (Zn^{2+})													
Optimised biochar (Zn-BC)	Zn^{2+}	10–300	1.5	5.5	25	240 min	Synthetic	Langmuir	Pseudo-2nd order	**208.47**	N/A	N/A	[92]

Note: C_0 = initial metal concentration; Dose = adsorbent dose; T = temperature; Matrix Type: all studies used synthetic single-metal solutions. C_0 values marked with an asterisk (*) were estimated from the isotherm range reported in the original study where the exact value was not explicitly stated. Like-for-like subset for Pb at pH ≈5, 25 °C, synthetic water: Cattle manure (CMB6) 40.8–51.87 mg/g; Sheep manure (SMB3) 20.2 mg/g; Palm kernel shell 7.48 mg/g; Bagasse 12.741 mg/g; Ca-modified (BC-Ca-P) 361.2 mg/g; Pine needle 40.4 mg/g. N/A = Not Applicable: the parameter was not reported by the source study, or is not applicable for the best-fit model (e.g., K_l is not applicable when Freundlich provides the best fit; K^f/n is not applicable when only Langmuir was fitted). Table 3 includes both unmodified (pristine) and modified biochars; modification status is identified in the Biochar Material column where stated by the source study. Direct comparison of q_{max} values across studies is only valid within comparable C_0, dose, and pH conditions.

Intraparticle Diffusion Model

The Weber-Morris model identifies diffusion as a rate-controlling mechanism:

$$q_t = k_{ip} \times t^{0.5} + C \quad \text{(Eq. 17)}$$

where k_{ip} = intraparticle diffusion rate constant (mg/g·min$^{0.5}$); C = boundary layer thickness constant (mg/g).

If the plot of q_t versus $t^{0.5}$ passes through the origin ($C = 0$), intraparticle diffusion is the sole rate-limiting step. Non-zero C values indicate boundary layer diffusion also contributes.

Although linearized forms of the Langmuir (Eq. 8) and pseudo-second order (Eq. 15) models are widely reported in the biochar literature for their computational convenience, they introduce systematic bias because linearization transforms the error structure of the original nonlinear equations. Parameter estimates obtained from linear regression on transformed data (e.g., C_e/q_e vs. C_e for Langmuir; t/q_t vs. t for pseudo-second order) can deviate substantially from those obtained by nonlinear least-squares regression applied directly to Eq. 7 and Eq. 14, respectively. Best practice is to apply nonlinear regression to the original model forms, report parameter uncertainty (95% confidence intervals or standard errors), and present the nonlinear R^2 or chi-squared (χ^2) goodness-of-fit alongside the fitted parameters. Where linearized fits are reported for comparative purposes, this should be explicitly stated.

How to Interpret These Models: Common Failure Modes

 doi:10.20944/preprints202605.1519.v1

Several interpretive pitfalls are common when applying these models to biochar adsorption data. (i) High R^2 does not confirm model validity. A high R^2 on a linearized fit is a necessary but not sufficient criterion for model selection; the nonlinear R^2 and chi-squared statistic should be reported, and multiple isotherm or kinetic models should be compared to identify the best fit. (ii) Pseudo-second-order dominance is partly an artifact of linearization. The near-universal reporting of pseudo-second-order fits in biochar studies partly reflects the mathematical robustness of the t/q_t linearization rather than genuine mechanistic evidence for chemisorption. A pseudo-second-order fit should not be interpreted as proof of chemisorption without corroborating spectroscopic or calorimetric evidence. (iii) R^aL and 1/n thresholds are concentration dependent. The Langmuir separation factor RL and the Freundlich heterogeneity parameter n are indicative of adsorption favourability only within the concentration range tested; extrapolating these conclusions beyond the experimental range is not justified. (iv) Intraparticle diffusion intercept must be reported. In the Weber-Morris model, reporting only the rate constant $k$ip without discussing the intercept C is incomplete. A non-zero C indicates that boundary layer (film) diffusion also contributes to the overall rate, and multi-linearity in the q_t vs. $t^{0.5}$ plot suggests sequential rate-limiting steps that should be resolved into their component stages.

4. Applications for Wastewater Treatment

4.1. Industrial Wastewater

Industrial wastewater streams often contain complex mixtures of heavy metals and recalcitrant organics, the treatment of which demands adsorbents capable of multi-modal contaminant removal. The characteristics of these streams are strongly influenced by the nature of industrial processes involved, such as metal finishing, mining, petrochemicals, dyes and pigment manufacturing, pharmaceutical formulation, and agrochemical production, and their effluents regularly present both high pollutant loads and a wide range of physicochemical conditions [8]. Such waters are likely to be enriched in toxic ions like Pb, Cd, Cr^{4+}, Ni, Cu, and Zn in combination with organics including dyes, phenolic compounds, nitroaromatics, or drug residues. In this context biochar offers a means to tackle multiple contaminant classes simultaneously through a combination of adsorption mechanisms. The porosity and heterogeneous surface chemistry of biochar permits uptake across these contaminant categories. Industrial discharge containing complex dyes, often coupled with metallic contaminants, has been effectively treated with biochar's derived from peanut hulls, sugarcane bagasse, and Murraya koenigii stems [21].

The microporous domains within such chars physically entrap dye molecules, while functional groups on the pore walls coordinate metal cations liberated during the same process. This dual action is particularly valuable for textile or printing effluents where colour removal alone fails to address toxicity arising from associated metals like chromium used in dye fixation. The relatively low production cost of agricultural residue-derived biochar further benefits large-scale applications common in these sectors. Chemical activation methods have been applied to tailor biochar for specific industrial wastewater challenges. Acid activation can enhance surface acidity and introduce oxygen-containing groups that are complex efficiently with divalent or trivalent metal ions prevalent in electroplating discharge [8]. Alkali activation can increase surface area while modifying surface potential to optimize Pb or Cd capture from battery manufacturing wastewaters. Both strategies support rapid mass transfer rates by ensuring unobstructed access to active sites even under high ionic strength conditions sometimes present in metallurgical waste streams. In effluents where heavy metals coexist with high concentrations of organic chelators, typical for tanning industries employing Cr salts, surface-bound mineral phases within biochar add another layer of remediation via precipitation mechanisms [2].

Phosphate-rich biochar's may induce the formation of insoluble lead or cadmium phosphates directly on the char surface. Similarly carbonate phases originating from plant feedstocks contribute to carbonate precipitation pathways beneficial for neutralizing acidic metalliferous drainage before

 doi:10.20944/preprints202605.1519.v1

final discharge. Industrial wastewater frequently exhibits extreme pH or redox conditions that can destabilize conventional sorbents. Biochar's relative structural resilience allows continued performance under such extremes. For example, mine leachates often emerge acidic and rich in Fe together with trace As; embedding iron oxides into biochar enhances its stability while also enabling redox transformations such as reduction of mobile As^{5+} to less soluble As^{3+} followed by adsorption [26]. Such Fe-loaded chars also display strong affinity for Cr^{6+} via simultaneous reduction-adsorption routes applicable to electroplating rinse waters. Performance optimization often involves coupling feedstock selection with industry-specific contaminant profiles. Grapevine waste-derived chars have displayed affinities for less polar compounds alongside the capacity for recovering polar species [101]. suggesting their utility where solvent-laden effluents mix with dissolved metals. In contrast, rice husk-based chars, with inherently high silica content, are mechanically stable under high-flow industrial channels yet still provide reactive silanol sites capable of coordinating certain transition metal species. A recurring challenge with industrial waste treatment is secondary pollution through adsorbent loss or leaching of modification agents. Magnetic functionalization circumvents some operational hurdles by allowing post-treatment recovery via magnetic separation rather than filtration. [26]. This simplifies operation at scale and reduces residual solids handling costs, an important economic consideration for facilities processing thousands of cubic meters per day. Another application angle involves retrofitting existing treatment systems. Biochar can replace or supplement activated carbon beds in tertiary polishing stages without substantial redesign because column hydrodynamics remain similar; however, due to feedstock variability it is possible to choose chars tailored toward specific problematic metals in the outflow from primary chemical treatments [14].

For instance, agricultural residue-based char modified with thiol groups could form part of a final-stage filter aimed specifically at mercury capture from chlorine-alkali plant wastewater. Industrial sludge itself, often generated as a byproduct of wastewater clarification, can be converted into value-added adsorbents through thermal activation routes [57]. Ash-rich sludges yield chars containing mineral matrices effective not only at capturing residual metals but also at nutrient recovery when effluents originate from fertilizer manufacture. This concept closes loops within industrial ecosystems by valorizing waste streams into process inputs for water treatment elsewhere on-site. Where wastewater composition varies temporally due to batch operations, as occurs in pharmaceutical formulation lines, biochar's broad-spectrum sorption acts as a buffer against concentration spikes that could overwhelm narrowly targeted treatment steps. Its integration into hybrid systems combining advanced oxidation (to degrade persistent organics) with biochar adsorption has shown promise against co-occurring micropollutants like antibiotics bound to metal ions [45]. Oxidative pre-treatment liberates ionic species from strong organic complexes which are then promptly immobilized by the char. Scaling industrial use inevitably raises questions about regeneration cycles and spent media management. Thermal reactivation may restore much adsorption capacity but must be weighed against energy costs and potential off-gassing of sequestered volatile organics [2].

Chemical regeneration using mild acid solutions can desorb certain cations without severely degrading pore structures; however, this must be tailored so as not to strip intended functionalization's critical for subsequent reuse batches. Field trials consistently point toward the need for system-specific optimization rather than generic substitution of adsorbent media [103]. Variability in flow rates, contaminant mixtures, temperature swings, and seasonal shifts can all impact contact times and equilibrium behaviour's within fixed-bed or fluidized reactors charged with biochar. Matching particle size distribution to reactor hydrodynamics prevents channeling losses while maintaining adequate porosity for deep penetration adsorption, a balance especially sensitive under continuous-operation regimes typical in industry. Ultimately the flexibility afforded by diverse biomass precursors combined with tunable production and modification pathways positions biochar as an adaptable tool across numerous industrial wastewater scenarios [2]. Whether embedded into multi-stage plants handling textile dye-metal co-contamination or deployed modularly at mining

 doi:10.20944/preprints202605.1519.v1

sites producing acid metalliferous drainage far from central facilities, engineered biochar's present a viable balance between performance demands and operational sustainability criteria that modern regulations increasingly impose on industry-wide water management practices [8].

4.2. Municipal Wastewater

Municipal wastewater contains a diverse range of contaminants arising from domestic sewage, stormwater inflows, and in some cases contributions from small-scale industrial activities. The chemical profile is often characterized by elevated organic matter, nutrients such as nitrogen and phosphorus, suspended solids, microorganisms including pathogens, and a variety of emerging pollutants like pharmaceuticals, personal care products, and synthetic dyes [8]. Heavy metals may also be present through diffuse sources including urban runoff, where brake wear releases copper or antimony particles, tyre abrasions shed zinc-rich dust, and leaching from household plumbing or fittings carrying lead alloys [102]. As discussed in previous sections (3.1 and 4.1), the challenge with multi-contaminant waste streams lies in designing treatment strategies that address simultaneous pollutant removal without sacrificing process efficiency. Biochar finds a particular niche here due to its ability to immobilize metallic species while interacting with organic molecules through different adsorption pathways. In municipal scenarios, biochar can be deployed as part of primary or tertiary treatment stages. Integrated into fixed-bed adsorption units downstream of biological treatments, it captures residual metals still dissolved after conventional processes such as activated sludge or trickling filters [104].

For example, Pb and Cu ions persisting post-secondary clarification can be sequestered within micro- and mesoporous structures while pharmaceuticals like diclofenac are retained through hydrophobic domain interactions [8]. The environmental benefit here extends beyond effluent purification; by trapping metals within stable carbon matrices prior to discharge, biochar hinders their accumulation in sediments where later remobilization might occur during storm events. The feedstocks selected for municipal applications often come from locally available biomass residues to ensure cost-effective supply chains and minimize the environmental footprint associated with transport [102]. Plant straw or sewage-derived biosolids converted via pyrolysis yield chars enriched in mineral components such as silica or calcium carbonate that contribute alternative removal mechanisms like metal precipitation. Biochar produced from biosolid precursors not only divert waste from landfill but transforms it into a functional adsorbent tailored for urban effluent conditions, closing material loops within municipal infrastructure. Such chars may exhibit higher ash content which is advantageous in immobilizing specific cations (e.g., Cd through carbonate precipitation), albeit at times reducing available surface area compared to wood-based counterparts [2].

Fixed-bed column setups using pristine biochar have displayed stronger performance in secondary-Treated wastewater compared to batch reactor formats [103]. Continuous flow maintains steep concentration gradients along the bed's length, sustaining high adsorption rates even under variable influent quality. However, modifications can improve efficiency further; acid-treated variants introduce carboxyl functionalities enhancing complexation with trivalent ions like Cr^{3+} prevalent where corroded infrastructure contributes chromium into the municipal network [30]. Magnetic biochars produced via $FeCL_3$ impregnation facilitate simple recovery post-treatment by magnetic separation, valuable within centrally managed facilities striving to decrease sludge contamination by spent media [105].

Municipal sewage systems increasingly contend with pharmaceutical residues whose persistence raises ecological concerns about antimicrobial resistance development [104]. Biochar's capacity to remove both inorganic metals and polar organics positions it well against such composite risks. For example, co-removal of antibiotics alongside Zn from laundry greywater entering the sewer system prevents synergistic toxicity effects on downstream microbial communities used in biological treatment processes. The porous structure provides retention space while polar surface sites attract hydrophilic drug molecules; concurrent ion exchange mechanisms secure the metal fraction [2]. Coupled biochar–constructed wetland systems offer another pathway for municipal application.

 doi:10.20944/preprints202605.1519.v1

Here biochar amendments within substrate beds improve acidity neutralization and foster stable plant growth while decreasing translocation factors for metals into wetland vegetation [106].

By immobilizing metals within wetland substrates rather than permitting uptake into biomass destined for disposal or reuse, these designs mitigate potential re-release into receiving waters. Moreover, nutrient cycling benefits emerge as biochar slows nitrate leaching, a relevant trait considering nutrient management obligations common at municipal level. Operational resilience is paramount when dealing with unpredictable pollutant spikes due to stormflow ingress or illicit discharges. Magnetic or composite-modified biochar's embedded into modular filtration units allow rapid deployment during episodic events without overhauling base infrastructure [32]. The magnetic property eases retrieval once contaminant loads normalize. Such adaptable capacity ensures continuity of service compliance without reliance on overbuilt centralized plants, particularly relevant in cities combining older sewer layouts with modern expansion areas. From an economic perspective, using locally sourced biomass for char production helps municipalities keep operational costs low relative to imported granular activated carbon [102]. In resource-limited contexts typical of smaller municipalities or peri-urban zones in developing regions, decentralized fixed-bed adsorbers filled with regionally produced char offer scalable solutions replicable near point-of-discharge locations rather than relying entirely on distant centralized facilities. This decentralization reduces hydraulic stress on main networks while integrating source control directly at sub-catchment levels. Regeneration practices must consider metal release risks back into treated effluents upon desorption. Mild acidic eluents can recover bound metals for recycling where economically viable (e.g., copper reclamation) while restoring active sites on the char for re-use cycles, important to reduce total life-cycle cost relative to single-use models [2]. Nevertheless, practical application requires balancing regeneration frequency against treatment continuity demands; some facilities might opt for periodic media replacement rather than onsite regeneration depending on scale and contaminant economics. By bridging affordability with multi-contaminant handling capability, including co-existing heavy metals and trace-level micropollutants, biochar expands the operational toolkit available to municipal water managers under tightening regulatory environments [104]. Its adoption aligns with circular economy principles referenced earlier through valorization of waste biomass streams while offering directly measurable improvements in effluent quality before discharge into natural receiving waters or reuse within reclaimed water programs.

4.3. Performance Evaluation and Optimization

4.3.1. Factors Affecting Removal Efficiency

Removal efficiency in biochar-based treatment systems is a function of multiple interacting variables, some inherent to the adsorbent material and others arising from environmental or operational conditions during application.

Removal efficiency (*RE*) expresses the percentage of contaminants removed from solution:

$$RE(\%) = \frac{(C_0 - C_e)}{C_0} \times 100 \qquad \text{(Eq. 18)}$$

where *RE* = removal efficiency (%); the percentage of contaminant removed from solution; C_0 = initial contaminant concentration (mg/L); C_e = equilibrium contaminant concentration in solution after adsorption (mg/L)

Among these, pH stands out as one of the most influential parameters. The ionization state of surface functional groups such as carboxyl (-COOH), hydroxyl (-OH), and phenolic moieties changes with pH, directly altering electrostatic interactions between the biochar surface and dissolved metal ions [14]. At low pH values, protonation of these groups results in a more positively charged surface which can repel cationic metals like Pb or Cd, thereby reducing adsorption efficiency. Conversely, under alkaline conditions deprotonation increases negative charge density, often enhancing uptake of positively charged species, although competing precipitation reactions may also occur within bulk solution, potentially diverting metals from sorption pathways toward sedimentation elsewhere.

 doi:10.20944/preprints202605.1519.v1

Temperature further modulates removal performance by influencing both kinetic and thermodynamic aspects of adsorption. Higher temperatures generally accelerate diffusion rates of solutes into internal pores; however, they can also weaken van der Waals forces important in physisorption [5]. For chemisorption-driven uptake, such as complexation or ion exchange, the enthalpy change can determine whether elevated temperatures favor stronger binding or initiate desorption processes. Biochars produced under varying pyrolysis temperature regimes therefore respond differently when introduced into treatment setups operating at disparate thermal conditions. The initial concentration of contaminants establishes the gradient driving adsorption dynamics [107]. Lower concentrations may see rapid attainment of equilibrium due to saturation of high-affinity sites without extensive mass transfer limitations; higher loads challenge site availability and can reveal the limits imposed by pore accessibility and total capacity. High initial metal content often produces steeper breakthrough curves in column operation unless adsorbent doses are scaled accordingly. Adsorbent dosage itself constitutes a direct control variable, greater amounts introduce more active sites and surface area to interact with contaminants, typically improving removal efficiency until diminishing returns set in as site redundancy emerges relative to the pollutant load [108].

Dosage increments must be balanced against hydraulic conductivity constraints since excessive packing can reduce flow rates through fixed-bed systems or alter suspension characteristics in batch reactors [46]. Contact time determines how thorough diffusion and binding processes proceed before effluent exits the treatment zone. Materials with complex hierarchical pore structures rely on adequate residence times for solutes to penetrate beyond mesopores into micropore regions where high-specific-area sites concentrate sorptive potential [16]. Short contact durations bias results toward external surface adsorption only; extended times encourage deeper interaction but at the risk of operational delays in high-throughput facilities unless system configuration accommodates longer retention without bottlenecks. The presence of co-existing ions alters effective capacity through competitive sorption or ionic strength effects [55]. In real wastewater streams, sodium (Na), potassium (K), magnesium (Mg), calcium (Ca), chloride, nitrate, and sulphate all vie for available binding sites. Some metal ions exhibit stronger affinities, often dictated by electronegativity differences or hydration energy, allowing them to displace weaker competitors. The resulting selectivity profiles depend heavily on functional group chemistry fixed within the char during production or imparted via modification treatments [16]. Increased ionic strength compresses electrical double layers around charged surfaces, which can reduce long-range electrostatic attraction yet foster localized ion clustering conducive to surface precipitation under certain chemistries. Feedstock origin imparts mineral compositions that influence specific removal mechanisms beyond electrostatic binding or physical entrapment [110].

A silica-rich rice husk char offers different interaction pathways compared to calcium-phosphate-containing bone char; the former might excel at structural stability under flow yet coordinate transition metals via silanol groups, whereas the latter drives carbonate precipitation with metals like Pb even in high-acidity environments. These intrinsic properties interact with operational parameters; acidic conditions may dissolve susceptible mineral phases prematurely while alkaline environments promote their reactivity toward targeted cations. Surface modifications amplify removal potential but also affect sensitivity to environmental variables [16]. Acid-functionalized chars maintain high performance over broader pH ranges by increasing density of reactive oxygen groups less prone to complete protonation shifts; magnetic iron oxide-loaded variants introduce both redox activity beneficial for conversion of toxic species (e.g., Cr^{4+} to Cr^{3+}) and operability benefits via magnetic retrieval post-use [30]. When combined with oxidants in integrated advanced oxidation systems, such materials exploit dual removal mechanisms wherein oxidative cleavage liberates metals from organic complexes followed by immediate capture on char surfaces [4].

Operational flow dynamics play a part as well. In continuous-flow reactors, uniform distribution prevents channeling that would bypass portions of packed beds, a problem intensified if particle size distributions are unevenly graded. Coarse particles improve hydraulic throughput but decrease total surface area; finer particles offer maximal contact but risk clogging under particulate-rich influents

 doi:10.20944/preprints202605.1519.v1

typical from pre-treatment lapses [46]. here influence not just immediate removal rates but also longevity across repeated cycles since mechanical attrition during flow impacts future capacity through particle loss or structural collapse. Finally, regeneration protocols directly feed back into observed removal efficiencies over multiple uses [2]. Regeneration methods capable of stripping bound metals without degrading core porosity preserve long-term functionality, a balance often difficult with aggressive acids that may remove embedded mineral phases central to precipitation-based capture routes. Thermal regeneration restores pore accessibility but consumes energy and could volatilize retained organics into unwanted emissions unless controlled carefully. Successive regeneration cycles inevitably modify surface chemistry whether intentionally or not; understanding these progressive changes inform realistic projections for field operation where adsorbents rarely operate in pristine first-use condition over extended lifespans.

To contextualize the discussion on adsorbent performance, Figure 5 compares the adsorption capacities of commonly used materials—pristine biochar, modified biochar, activated carbon, highly modified/composite biochar, and ion exchange resin—alongside their regeneration capability. The data are drawn from representative studies and illustrate the relative efficiency of each adsorbent under typical conditions for Pb^{2+}. removal. While composite (Fe–Mn oxide–modified) biochar exhibits the highest adsorption capacity, all materials share a common limitation in regeneration, reflecting practical challenges in maintaining long-term functionality.

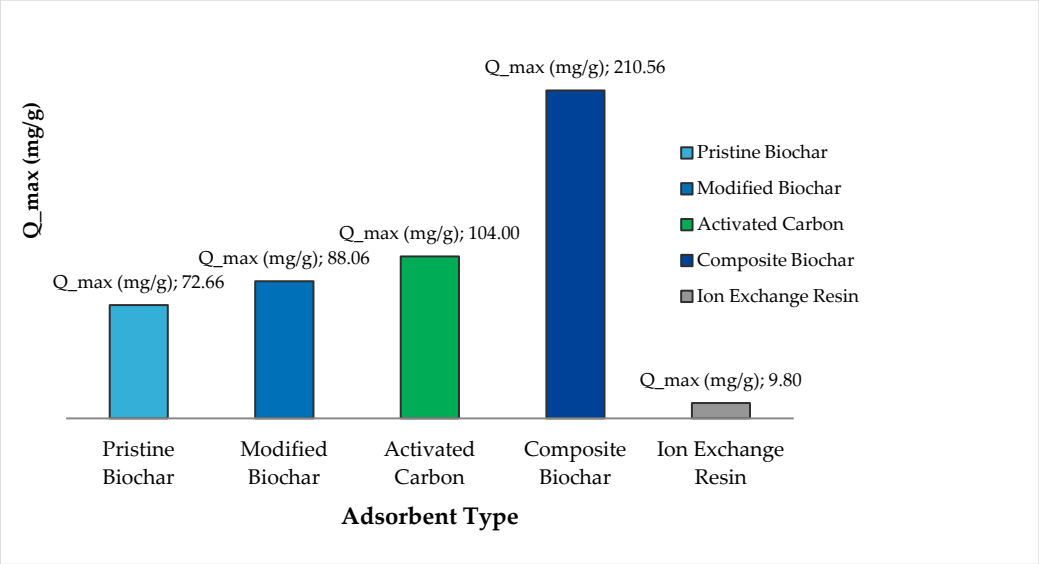

Figure 5. Comparative Adsorption Capacity and Regeneration Capability of Common Adsorbents for Pb^{2+}. Note: q_{max} values are drawn from five independent studies [111–115] conducted under different experimental conditions, including varying initial Pb^{2+}. concentrations, adsorbent doses, solution pH, contact times, and temperatures. Because these variables directly influence q_{max}, the values presented are not directly comparable on a quantitative basis. The figure is intended to illustrate indicative performance trends across adsorbent categories rather than to provide a controlled like-for-like comparison.

Thermodynamic Parameters

Thermodynamic parameters, including enthalpy change (ΔH°), entropy change (ΔS°), and activation energy (Ea), provide critical insights into the spontaneity, energy requirements, and temperature-dependence of metal adsorption processes on biochar surfaces. Thermodynamic analysis determines the entropy variations during adsorption.

Gibbs Free Energy Change

$$\Delta G^{\circ} = -RT\ln K_d \qquad \text{(Eq. 19)}$$

 doi:10.20944/preprints202605.1519.v1

where ΔG° = Gibbs free energy change (kJ/mol); R = universal gas constant (8.314 J/mol·K); T = absolute temperature (K); Kd = distribution coefficient (L/g).

The distribution coefficient is:

$$K_d = \frac{q_e}{C_e} \quad \text{(Eq. 20)}$$

Negative ΔG° values indicate spontaneous adsorption; positive values suggest non-spontaneous processes.

Enthalpy and Entropy Changes

The relationship between ΔG°, enthalpy change (ΔH°), and entropy change (ΔS°) is:

$$\Delta G° = \Delta H° - T\Delta S° \quad \text{(Eq. 21)}$$

The Van't Hoff equation relates temperature to thermodynamic parameters:

$$\ln K_d = -\frac{\Delta H°}{RT} + \frac{\Delta S°}{R} \quad \text{(Eq. 22)}$$

Plotting ln K_d versus 1/T yields a straight line with slope = -ΔH°/R and intercept = ΔS°/R.

Interpretation:

- Negative ΔH° indicates exothermic adsorption; positive ΔH° indicates endothermic
- Positive ΔS° suggests increased randomness at the solid-solution interface
- ΔH° values < 40 kJ/mol suggest physical adsorption; > 40 kJ/mol indicate chemisorption

Activation Energy

The Arrhenius equation relates the rate constant to temperature and activation energy:

$$k = A\exp\left(-\frac{E_a}{RT}\right) \quad \text{(Eq. 23)}$$

Linearized form:

$$\ln k = \ln A - \frac{E_a}{RT} \quad \text{(Eq. 24)}$$

where k = rate constant; A = Arrhenius constant (frequency factor); Ea = activation energy (kJ/mol).

Activation energy values < 40 kJ/mol typically indicate physical adsorption; values between 40-800 kJ/mol suggest chemisorption. Table 4 presents the thermodynamic properties of some biochar biosorption of metals with positive entropy changes.

In addition to the distribution coefficient (K_d) used in Equation 20, a comprehensive thermodynamic analysis of biochar adsorption systems should incorporate the full suite of equilibrium-based parameters. The Langmuir maximum adsorption capacity (q_{max}, mg/g) and Langmuir affinity constant (K_L, L/mg) quantify monolayer binding on homogeneous surfaces, while the Freundlich constants K_F and 1/n characterize adsorption intensity on heterogeneous surfaces. Together with the van't Hoff-derived ΔH° and ΔS° and the Arrhenius-derived activation energy (Ea), these parameters provide a mechanistically complete thermodynamic description of the adsorption process. For example, Koprivica et al. [110] reported Langmuir, Freundlich, Sips, and Redlich–Peterson isotherm constants alongside ΔG°, ΔH° = +149.47 kJ/mol, and ΔS° = +586.92 J/(mol·K) for Pb^{2+} removal by NaOH-activated Paulownia-leaf hydrochar, demonstrating that positive entropy change and spontaneous (negative ΔG°) adsorption can co-occur under endothermic conditions – a finding directly relevant to the biochar systems reviewed here [109].

Table 4. Thermodynamic parameters of Metal biosorption on Biochar.

Biochar	Metal	ΔH° (kJ/mol)	ΔS° (J/mol·K)	Es (kJ/mol)	Reference
Corn stalk biochar - Raw Carbon (RC)	Cr^{6+}	15.24	67.31	N/A	[116]

 doi:10.20944/preprints202605.1519.v1

Corn stalk biochar - Organic Component (OC)	Cr^{6+}	13.92	63.64	N/A	[116]
Corn stalk biochar - Inorganic Component (IC)	Cr^{6+}	10.57	50.91	N/A	[116]
Activated carbon from co-mingled wastes	Cr^{3+}	3-11	Positive	60	[116]
Norit activated carbon (oxidized)	Cr^{3+}	N/A	Positive	92	[116]
Konjac starch hydrophilic carbon spheres (HCSs-2)	Pb^{2+}	18.65	87.17	N/A	[117]
Magnetic biochar/MgFe-LDH composite	Pb^{2+}	Endothermic	Positive	N/A	[118]
Modified reed biochar (MRBC)	Pb^{2+}	Endothermic	Positive	N/A	[65]
Tea waste biochar composite (CMCB@TWBM/ZIF-67)	Pb^{2+}	-76.724	N/A	<8	[119]
Nitrogen-purged biochar (NPBC)	Pb^{2+}	-16.32 to -19.37	Positive (3.45-8.56)	N/A	[119]
Steam-activated biochar (SABC)	Pb^{2+}	-15.59 to -18.62	Positive (9.97-11.13)	N/A	[117]
Konjac starch carbon spheres	Cd^{2+}	Endothermic	Positive	N/A	[120]
Euhalophyte biochar (SBC)	Cd^{2+}	Negative (exothermic)	N/A	N/A	[120]
Maize biochar (ZBC)	Cd^{2+}	Positive (endothermic)	N/A	N/A	[65]
Tea waste biochar composite (CMCB@TWBM/ZIF-67)	Cd^{2+}	-61.664	N/A	<8	[119]
Nitrogen-purged biochar (NPBC)	Cd^{2+}	-10.53 to -16.34	Positive (15.34-22.56)	N/A	[119]
Steam-activated biochar (SABC)	Cd^{2+}	-9.87 to -14.21	Positive (18.45-25.67)	N/A	[121]
Beech biochar (pyrolyzed at 400-700°C)	Cd^{2+}	N/A	N/A	151-184	[121]
Spruce biochar (pyrolyzed at 400-700°C)	Cd^{2+}	N/A	N/A	157-172	[121]
Beech biochar (pyrolyzed at 400-700°C)	Cu^{2+}	N/A	N/A	151-184	[121]
Spruce biochar (pyrolyzed at 400-700°C)	Cu^{2+}	N/A	N/A	157-172	[122]
Biochar-humic acid system (BS-HA)	Cu^{2+}	Endothermic	Positive	8.0-16.0 (E)	[136]
Macadamia nutshell magnetic biochar (MCA-BC)	Cu^{2+}	Positive (heat-absorbing)	Positive (entropy-increasing)	N/A	[124]
Lemonwood biochar modified with zeolite/alginate/Fe_3O_4	Zn^{2+}	Endothermic	Positive	N/A	[125]
Hardwood biochar	Ni^{2+}	Slightly endothermic	N/A	N/A	[125]

 doi:10.20944/preprints202605.1519.v1

Softwood biochar	Ni^{2+}	Slightly endothermic	N/A	N/A	[125]
Hardwood biochar	Zn^{2+}	Slightly endothermic	N/A	N/A	[125]
Softwood biochar	Zn^{2+}	Slightly endothermic	N/A	N/A	[125]
Arundo donax biomass (Cd-loaded)	Cd^{2+}	N/A	N/A	Reduced by 1.85-3.84	[126]
Broussonetia papyrifera (Cd-loaded)	Cd^{2+}	N/A	N/A	Reduced by 0.93-13.28	[126]

4.4. Biochar in Hybrid and AOP-Integrated Treatment Systems

Biochar occupies two mechanistically distinct roles in hybrid treatment configurations: a passive adsorbent that concentrates contaminants at its surface, and an active catalyst or electron-transfer mediator that drives chemical transformation of those contaminants in situ. Conflating these roles (or asserting catalytic synergy without mechanistic evidence) is a recurring weakness in the literature that this section addresses by separating adsorption-dominant from catalysis-dominant hybrid systems, grounding each in reported operating conditions and performance metrics, and distinguishing laboratory batch evidence from pilot- or field-scale demonstrations. Table 5 summarises representative hybrid systems reported in the literature across these two categories.

Table 5. Representative Biochar Hybrid and AOP-Integrated Systems for Heavy Metal Removal.

System / Biochar Type	Category	Target Metal / Speciation	Key Operating Conditions	Reported Performance	Scale	Ref.
Biochar fixed-bed post-secondary biological treatment	Adsorption + biological	Pb^{2+}, Cd^{2+}, Cu^{2+}; dissolved ionic fraction	Column; secondary effluent matrix; neutral pH; ambient T	Extended breakthrough vs. raw influent; residual metal removal >80% in secondary effluent	Lab/pilot column	[1,100].
Biochar–constructed wetland (5–10% w/w substrate amendment)	Adsorption + wetland	Pb^{2+}, Cd^{2+}; ionic + particle-bound fractions	Mesocosm; controlled hydraulic load; pH 6–7; 25°C	60–85% reduction in dissolved Pb^{2+}/Cd^{2+} vs. unamended control; reduced metal translocation into wetland biomass	Mesocosm (lab)	[102]
Fe-modified biochar (Fe-BC) + H_2O_2 (Fenton-like)	Adsorption + Fenton AOP	Co-occurring organics + Pb^{2+}/Cd^{2+} (indirect AOP benefit)	Batch; pH 3–5; H_2O_2 10–50 mM; Fe-BC 0.3–1 g/L; 25°C; 60–120 min	Organic co-contaminant degradation >85%; metals captured post-oxidation; Fe leaching 0.1–2 mg/L per cycle	Lab batch	[127]

 doi:10.20944/preprints202605.1519.v1

Fe-BC / nZVI-BC + persulphate or peroxymonosulphate (PS/PMS)	Catalytic AOP (SR-AOP)	Organics (antibiotics, dyes); indirect heavy metal liberation	Batch; pH 3–7; PS/PMS 1–5 mM; catalyst 0.5–2 g/L; 25°C; 30–120 min	SO_4^{-} generation confirmed by EPR; >90% organic removal in synthetic solution; matrix scavenging reduces efficiency in real wastewater	Lab batch	[128]
Fe-BC / nFeS-BC: simultaneous Cr^{6+} reduction–adsorption	Catalytic redox + adsorption	$Cr^{6+} \rightarrow Cr^{3+}$; reduction + surface immobilization	Batch; pH 1–3; C_0 10–500 mg/L; 0.5–2 g/L adsorbent; 25°C; 240–1440 min	q_{max} 66–435 mg/g (pH- and Fe-loading-dependent); Cr^{3+} confirmed by XPS; Fe^{2+} consumption quantified	Lab batch	[92,93,129]
Mn-Fe oxide/biochar composite (MBC-MFC)	Catalytic redox + adsorption	Cr^{6+} + total Cr; surface complexation + electrostatic attraction	Batch; pH 3; 25°C; 48 h; dose 0.1 g/50 mL; SSA 318.5 m^2/g	q_{max} 56.2 mg/g Cr^{6+}; 4.16× improvement over unmodified biochar; regenerated with 0.3 M NaOH ×5 cycles	Lab batch	[130]
nZVI/biochar fixed-bed (permeable reactive barrier)	Catalytic redox + column	Cr^{6+}; reductive immobilization	Fixed-bed column; variable bed heights; pH 2–6; continuous flow	Total Cr to 0 mg/L outlet; breakthrough modelled by Thomas/ANN; performance stable across bed heights	Lab column	[76]

Notes: All entries are from batch or column laboratory experiments unless stated. Scale: Lab batch = synthetic solution, single-pass batch reactor; Lab/pilot column = packed-bed column with controlled flow; Mesocosm = outdoor or greenhouse wetland mesocosm. NR = Not Reported. SR-AOP = sulphate radical-based advanced oxidation process. qmax = maximum Langmuir adsorption capacity. SSA = BET specific surface area.

Adsorption-Dominant Hybrid Systems

In adsorption-dominant hybrids, biochar serves primarily as a sorbent while a co-process (biological treatment, coagulation, or constructed wetland) handles complementary removal pathways. The most thoroughly characterised configuration couples biochar fixed-bed columns with secondary biological treatment: biochar placed downstream of activated sludge captures residual dissolved metals (Pb^{2+}, Cd^{2+}, Cu^{2+}) and co-occurring pharmaceuticals not degraded biologically, while the biological stage pre-treats bulk organics that would otherwise compete for biochar binding sites.

 doi:10.20944/preprints202605.1519.v1

Published lab-scale and pilot-scale column data consistently show that placing biochar post-secondary treatment extends breakthrough times significantly compared to direct application to raw influent, because the lower organic load in secondary effluent reduces competitive sorption. [1,100]. Constructed wetland–biochar systems represent a second well-evidenced configuration: biochar amended into wetland substrate at 5–10% w/w has been shown in mesocosm studies to decrease metal translocation into wetland biomass, improve substrate hydraulic conductivity, and reduce dissolved Pb^{2+} and Cd^{2+} in outflow by 60–85% relative to unamended controls. [102] The biochar role here is unambiguously adsorptive, and the synergy with the wetland system is physical (improved flow distribution) and chemical (immobilization at the substrate level rather than in the water column). It is important to note that all constructed wetland–biochar performance data currently available are from batch and mesocosm experiments under controlled hydraulic loading; no peer-reviewed pilot or field-scale demonstration over more than one year has been published for combined heavy metal and emerging contaminant removal, representing a critical evidence gap before these systems can be recommended for full-scale deployment. [102]

Catalysis-Dominant Hybrid Systems: Biochar-AOP Integration

When biochar is loaded with redox-active metals – most commonly Fe^{2+}/Fe^{3+} species (Fe-BC), MnO_2, or nanoscale zero-valent iron (nZVI) – it transitions from a passive adsorbent into an active catalyst capable of driving AOP reactions. Three mechanistically distinct catalytic pathways are operative in these systems, and they must be distinguished clearly: (i) Fenton and Fenton-like reactions, in which Fe^{2+} embedded in the biochar matrix activates H_2O_2 to generate hydroxyl radicals (OH) that degrade co-occurring organic contaminants; (ii) persulphate/peroxymonosulphate (PS/PMS) activation, in which transition metals on the biochar surface cleave the O–O bond of the oxidant to generate sulphate radicals (SO_4^-), which exhibit greater selectivity and longer half-lives than OH; and (iii) direct electron-transfer reduction, in which Fe^{2+} or persistent free radicals (PFRs) on the biochar surface donate electrons directly to Cr^{4+}, reducing it to less toxic and less mobile Cr^{3+} without requiring an external oxidant. The third pathway is the most relevant for heavy metal speciation control and has the strongest mechanistic evidence base from characterization studies using X-ray photoelectron spectroscopy (XPS) and electron paramagnetic resonance (EPR) spectroscopy. [127,128]

For Cr^{4+} removal specifically (the metal for which the evidence hierarchy is strongest) the operative mechanism in Fe-BC systems follows a sequential reduction–adsorption pathway: Cr^{4+} is first electrostatic-attracted to the positively charged biochar surface under acidic conditions (optimal pH 2–3), then chemically reduced by surface Fe^{2+} or PFRs to Cr^{3+}, and finally the Cr^{3+} product is immobilized by surface complexation or precipitation as $Cr(OH)_3$. This three-step sequence has been confirmed by XPS analysis of post-reaction char surfaces, which show the emergence of Cr^{3+} peaks and the consumption of Fe^{2+} species. [85,86,126] Reported Cr^{3+} removal capacities in Fe-BC batch systems range from 66 to >435 mg/g depending on Fe loading, pH (typically 1–3), initial concentration (10–500 mg/L), temperature (25°C), and contact time (240–1440 min) – the wide spread in these values is entirely attributable to differences in operating conditions, confirming that single-point q_{max} values from Langmuir fitting cannot be compared across studies without condition matching. For Pb^{2+} and Cd^{2+}, the catalytic role of biochar is less prominent; removal proceeds primarily through adsorption (complexation, ion exchange, precipitation), with the AOP contribution being indirect – oxidative pre-treatment liberates metal ions from chelating organic ligands, increasing the free ionic fraction available for biochar capture. [45,127,128].

Regarding demonstrated stability in hybrid AOP systems, virtually all published data are from batch experiments at lab scale. The key performance metrics that should be reported (but are frequently absent) are: (i) catalyst stability over multiple reaction cycles, specifically whether Fe leaching from the biochar matrix remains below regulatory limits for Fe in treated effluent; (ii) radical scavenging by wastewater matrix constituents (carbonate, sulphate, humic substances), which compete with target contaminants for OH or SO_4^- and substantially reduce effective radical

 doi:10.20944/preprints202605.1519.v1

concentrations under real wastewater conditions compared to synthetic solutions; and (iii) the fate of oxidation by-products from the AOP stage, particularly for systems targeting mixed organic–metal streams where partial oxidation can generate toxic intermediates more harmful than the parent compounds. At present, no peer-reviewed pilot-scale study of an Fe-BC/AOP hybrid system for simultaneous heavy metal and organic co-contaminant removal from real industrial wastewater over sustained operation (>100 h) has been identified in the literature. This constitutes the primary scale-up evidence gap for AOP-biochar hybrid systems. Claims of "catalytic synergy" should therefore be explicitly qualified as laboratory batch observations requiring pilot validation before they can be translated into design parameters for treatment systems. [127,128]

4.5. Regeneration and Reusability of Biochar

Maintaining biochar's adsorption performance over extended operational lifespans depends on regeneration approaches that restore active sites without compromising structural integrity.

Regeneration Efficiency

$$RE_{reg}(\%) = \frac{q_{e,n}}{q_{e,1}} \times 100 \quad \text{(Eq. 25)}$$

where $q_{e,n}$ = adsorption capacity after nth regeneration cycle; $q_{e,1}$ = initial adsorption capacity.

Desorption Efficiency

$$DE(\%) = \frac{C_d \times V_d}{q_e \times m} \times 100 \quad \text{(Eq. 26)}$$

where C_d = desorbed metal concentration (mg/L); V_d = volume of desorption solution (L).

Following a treatment cycle, the active binding domains, functional groups, mineral phases, and internal pore surfaces, often become saturated with heavy metals or other adsorbates. Without adequate regeneration, subsequent reuse can lead to progressive capacity loss due to site blockage, competition effects, and chemical deactivation [132]. In practice, regeneration can follow several pathways: thermal, chemical, physical, or biological treatments, each with distinct efficiency profiles and operational trade-offs. Thermal regeneration is widely regarded as an effective technique for removing adsorbed species by increasing temperature to drive desorption and oxidative cleaning of the carbon matrix. Applying steam, inert gases like nitrogen, hot water vapour, or microwave energy induces volatilization or decomposition of bound contaminants [131]. Higher temperatures favour complete removal of residual adsorbates but may risk altering surface chemistry, especially the oxygen-containing functional groups responsible for cation binding, if not controlled carefully. For certain feedstocks rich in volatile minerals or functionalized phases introduced during modification, excessive heating can degrade the attributes underpinning metal uptake capacity in later cycles. Chemical regeneration employs solutions such as acids (HCl, HNO), bases (NaOH), salts (NaNO, KNO, CaCl), or chelating agents to disrupt adsorbent–contaminant bonds and flush retained ions from pores [16].).

Selection of reagents must balance effectiveness against the potential for deterioration of the biochar framework; strong acids can remove mineral co-factors beneficial for precipitation pathways while high-pH treatments might erode microstructure over repeated uses. Solvent regeneration, using chemicals like methanol or supercritical fluids, offers targeted removal mechanisms for certain organic-bound metals where polarity tuning enhances selectivity [4]. Cost-effectiveness remains a concern; reagents should be inexpensive enough for routine use yet compatible environmentally when considering disposal after desorption. Physical regeneration strategies such as washing with clean water or filtration can clear loosely bound particulates and some ionic species but generally lack the potency needed to recover full adsorption capacity from heavily loaded media [16]. However, when paired with mild chemical rinses they contribute to maintenance between full-scale regenerations by removing surface fouling before it becomes irreversible. Biological processes

 doi:10.20944/preprints202605.1519.v1

present more novel approaches: microorganisms capable of metabolizing organic co-contaminants could indirectly liberate metal-binding domains within biofilm-laden biochar matrices by digesting obstructive residues. While promising theoretically, operational control is more complex given microbial community dynamics in wastewater environments. The choice of regeneration method often hinges on original feedstock properties and applied modifications. Acid-functionalized chars are more resilient under low-pH chemical regenerations compared to untreated plant-derived biochars whose mineral phases might dissolve when exposed repeatedly to strong acids [132].

Magnetic biochars containing FeO inclusions exhibit stable capacity retention after acid washing due to mechanical robustness and minimal leaching of embedded magnetic particles; these features also permit easier separation during regeneration processes where physical manipulation is necessary [16]. Reusability metrics combine percentage recovery of initial capacity per cycle with total number of viable cycles before replacement becomes necessary. Some studies demonstrate minimal reduction after multiple cycles using tailored regenerants, for example HCl treatment restoring near-original Pb^{2+} uptake capacities over several rounds [132], while others report marked declines attributable to precipitation within pores or deactivation of reactive groups from prolonged contaminant exposure. Structural degradation from repeated thermal swings may enlarge pore sizes beyond optimal thresholds for certain ion sizes; likewise chemical scouring can strip away modification layers painstakingly added during activation stages. Optimizing regeneration requires considering contaminant type specificity. Pb bound through carbonate precipitation may be released efficiently under acidic washes that dissolve carbonate phases whereas metals held via strong inner-sphere complexes may require chelating agents that address coordination stability directly [16]. Industrial wastewaters bearing mixed metals complicate this further since multi-element sorption creates overlapping binding scenarios where universal regenerants risk partial recovery only. Economic viability depends on extending sorbent lifespan relative to procurement and processing costs. Every avoided replacement cycle reduces resource consumption and waste generation while lowering operational expenditure in continuous treatment plants [131]. Effective regeneration thus aligns both environmental and fiscal imperatives; regenerating spent media minimizes solid waste disposal volumes and recycles captured metals if recovery streams are implemented. Valuable metals like copper reclaimed from biochar eluates could be re-integrated into production loops. From an environmental management standpoint, regeneration also mitigates secondary pollution risks associated with discarding heavy metal-laden sorbents without stabilization [18].

Designing closed-loop systems where desorbed metals are isolated for recycling enhance overall sustainability while satisfying regulatory constraints on hazardous waste handling. Hydrochar systems face parallel challenges: their lower aromaticity compared to pyrolytic chars makes them more vulnerable to structural impacts from aggressive regenerants [11]. Developing gentle yet effective methods remain important in preserving mechanical strength alongside adsorption performance; research points toward environmentally friendly reagents and combined mild-thermal protocols as potential pathways. Overall success in biochar reusability depends on understanding how repeated recovery techniques alter surface chemistry and porosity over time, knowledge enabling predictive models for long-term field performance rather than short-term lab trials alone [16]. Adaptive strategies could vary regenerant type across cycles based on evolving sorbent properties following each use phase, preventing premature performance collapse in systems expected to run continuously over months or years. Table 6 presents the conditions of regeneration and reusability of biosorption of metals on different biochars. The long-term sustainability and economic viability of biochar as an adsorbent depend critically on effective regeneration strategies that restore adsorption capacity while maintaining structural integrity across multiple treatment cycles.

Table 6. Conditions of Regeneration and Reusability.

 doi:10.20944/preprints202605.1519.v1

Biochar	Metal	Regeneration Agent	Number of Regeneration Cycles	Capacity retention (%)	Key stability observation	References
Magnetic biochar/MgFe-LDH (LMBC)	Pb^{2+}	2 M NaOH	5	~70% (from 83% to ~58%)	Slight decrease in each cycle	[133]
$MgCl_2$-modified biochar	Pb^{2+}	NaOH	5	75%	25% reduction in capacity after 5 cycles	[132]
Nitrogen-phosphorous modified biochar	Pb^{2+}	NaOH/HCl	4	>95%	Only slight decrease after 4th cycle	[132]
Silicate magnetic biochar sphere (SMBCS)	Pb^{2+}	EDTA-2Na + ultrasound	3	~73.4%	Pb removal: 26.6% reduction over 3 cycles	[134]
Magnetic biochar with graphene (MBCG)	Cd^{2+}	0.3 M HNO_3 + 0.03 M NaOH	5	92.1%	Consistent regeneration capacity maintained	[133]
Biochar with graphene (BCG)	Cd^{2+}	0.3 M HNO_3 + 0.03 M NaOH	5	21.6%	Dramatic decline (78.4% loss by 5th cycle)	[133]
Modified biochar	Cd^{2+}	0.1 M HNO_3	3	High desorption	First and third cycle show stable efficiency	[133]
Paper mill sludge biochar	Cd^{2+}	0.5 M NaOH	3	N/A	100% desorption in 36 hours	[133]
Silicate magnetic biochar sphere (wheat-straw derived) (SMBCS)	Cd^{2+}	EDTA-2Na + ultrasound	3	~71.4%	Cd removal: 28.6% reduction over 3 cycles	[134]
Chitosan/magnetic biochar composite (MWSBC-0.5)	Cr^{6+}	HCl (protonation)	7	Residual performance 78.6% after 7 cycles	Multilayer composite exposes fresh layers; enhanced reusability compared to typical chitosan-composites	[135]
Chitosan-modified magnetic bamboo biochar (CMBB)	Cr^{6+}	Acid/base (HCl/NaOH) cycles	5	>90% adsorption efficiency retained by CMBB; MBB <50%	Broader pH tolerance (2–10); improved recyclability vs. unmodified magnetic biochar	[123]
nFeS-modified biochar (fixed-bed system)	Cr^{6+}	Chemical elution	5	≈50% of initial	Two-stage system (nFeS-	[76]

 doi:10.20944/preprints202605.1519.v1

		(study protocol)		capacity retained after 5 cycles	BC + CTAB-BC) reduces total Cr to 0 mg/L; retention quantified under dynamic flow	
Bagasse-derived magnetic biochar (BMBC)	Cr^{6+}	0.2 M NaOH	3	80.4% removal efficiency after 3 cycles	Crystalline Fe_3O_4 structure retained; magnetic properties maintained	[140]
nZVI-modified sludge biochar (TP-nZVI/BC)	Cr^{6+}	Fixed-bed eluent (not specified)	—	Regenerative performance shown (breakthrough curves reported)	Performance stable across bed heights and concentrations; modelled by Thomas/ANN	[136]
Agro-waste peanut husk MgO biochar (nMgO@GHBC)	Cr^{6+}	NaOH, HNO3, H2SO4, EDTA	10	Reusable up to 10 cycles (described)	Sustained fixed-bed performance; 50 mg/g capacity	[137]
Magnetic biochar functionalized with chitosan–EDTA (E-CMBC)	Pb^{2+}	EDTA	3	97.26% adsorption capacity retained; 78.60% sorbent recovered	Strong complexation via amide/carboxyl groups; magnetic separation (3.1 emu/g)	[139]
N-doped chitosan biochar (OCS-160)	Cr^{6+}	NaOH	4	55% (from 190.48 to 105 mg/g)	Good regeneration with cycling performance	[135]
$FeCl_3$-modified corn stalk biochar (FeMB)	Cr^{6+}	NaOH	5	50% (from 91.91% to 46%)	First cycle: 97%, then gradual decline	[141]
HCl-modified biochar (HMB)	Cr^{6+}	NaOH	5	38% (from 47.99% to 18.29%)	29.69% reduction in removal rate	[141]
NaOH-modified biochar (NaMB)	Cr^{6+}	NaOH	5	38.5% (from 91.91% to 35.42%)	56.48% reduction in removal rate	[141]
Nano-FeS biochar composite (nFeS-BC)	Cr^{6+}	NaOH	5	50%	Retained 50% of initial capacity	[142]

 doi:10.20944/preprints202605.1519.v1

Amide-modified rice husk biochar (ABC)	Cr^{6+}	0.1 M NaOH	5	~60%	NaOH most effective regenerant	[143]
Mulberry stem biochar/Mn-Fe composite (MBC-MFC)	Cr^{6+}	0.3 M NaOH	5	Stable	Better desorption than HCl	[133]
Silicate magnetic biochar sphere (SMBCS)	As	EDTA-2Na + ultrasound	3	~57.1%	As removal: 42.9% reduction over 3 cycles	[134]
Magnetic biochar (thermal regeneration)	Various metals	Thermal (300°C)	3	62-64%	Followed by 0.1M NaOH desorption	[144]
Magnetic biochar (microwave regeneration)	Various metals	Microwave (900W)	3	Increasing with cycles	Better magnetic properties after 2nd & 3rd cycles	[144]
Water-hardened magnetic composite biochar spheres (WMBCS)	Cd, Pb, As	EDTA-2Na (shaking + ultrasound)	5	Regeneration efficiency 92.3–95.4% over 5 cycles; adsorption efficiencies maintained (Cd 26.5–30.6%, Pb 25.4–30.2%, As 30.2–41.0%)	Low mass loss (7.6%); low Fe leaching (~475 mg/kg); magnetic separation efficiency 98.8–99.8%	[134]
Engineered biochar nanocomposite (lemonwood-derived, zeolite/alginate/magnetic NPs)	Zn^{2+}, Cu^{2+}, Cd^{2+}	Acidic desorption (not specified in abstract)	3	No considerable loss of adsorption capacity across 3 cycles	Pseudo-second-order kinetics; exothermic & spontaneous adsorption; reusable	[124]

4.6. Mass Balance, Secondary Waste Streams, and Regeneration Performance Distributions

A critical but underexamined dimension of biochar regeneration is its mass balance: the regeneration step does not eliminate contaminants but transfers them from a solid phase (spent biochar) into a liquid phase (the spent regenerant solution). This phase transfer creates secondary waste streams whose management determines the true environmental benefit of biochar-based treatment. Spent acid or base regenerants contain concentrated metal ions (for example, HCl eluates from Pb^{2+}-loaded biochar may carry metal concentrations several orders of magnitude above the original influent) and require either further treatment (e.g., electrodeposition, precipitation, or ion exchange) or controlled disposal under hazardous waste regulations. Where metal concentrations are economically viable, closed-loop recovery is preferable: copper reclaimed from EDTA-regenerated eluates, for instance, can re-enter industrial production circuits, converting a waste liability into a resource stream. Chelating regenerants such as EDTA or Na_2EDTA introduce their own long-term leaching concerns if residual chelating agent remains sorbed within biochar pores after washing, as these ligands can remobilize trace metals during subsequent adsorption cycles. Similarly, thermally

 doi:10.20944/preprints202605.1519.v1

regenerated chars risk off-gassing of volatile organics co-adsorbed alongside metals, necessitating off-gas capture systems at scale. Stability against long-term leaching – particularly of inherent heavy metals present in the feedstock ash (e.g., Cd, Pb, and As in sewage sludge-derived chars) – must be evaluated via toxicity characteristic leaching procedure (TCLP) or equivalent standardised protocols before spent biochar is classified for land disposal. Without these mass balance and leaching assessments, regeneration studies report only half the environmental picture: high RE% values cannot be interpreted as sustainability outcomes unless the fate of the desorbed contaminant mass is also accounted for.

Synthesizing the regeneration data compiled in Table 6 as a performance distribution, rather than as isolated case studies, reveals several system-level patterns. Across all 28 entries in Table 6 spanning six metal classes (Pb^{2+}, Cd^{2+}, Cr^{6+}, Cu^{2+}, Zn^{2+}, and As), the median capacity retention after five regeneration cycles is approximately 70–78%, with a wide interquartile range from ~50% (e.g., nano-FeS biochar composites, HCl-modified biochars) to ~92–95% (e.g., EDTA-functionalized magnetic biochars, chitosan–magnetic composites). This distribution highlights that modification strategy is a stronger predictor of reusability than metal type or regenerant class alone. Bifunctional and magnetically modified biochars consistently cluster in the upper quartile of capacity retention, retaining >90% after five cycles in multiple studies [134,139], whereas single-reagent-modified biochars (NaOH or HCl only) tend toward 38–75% retention, with more variable decline profiles. Cycle-by-cycle trajectories also differ qualitatively: composites with multilayer structures (e.g., chitosan/magnetic bamboo biochar, CMBB) show near-linear retention, losing <2% per cycle, while simpler modified biochars often display a steeper initial loss in cycles 1–2 followed by a plateau, suggesting rapid loss of weakly bound surface functionalities early and stabilization once only strongly coordinated sites remain. These distributional insights are practically important: median performance at five cycles (rather than best-case performance at one or two cycles) is the operationally relevant benchmark for cost modelling of sorbent replacement intervals. Future regeneration studies should adopt a minimum reporting standard of five adsorption–desorption cycles, report cycle-by-cycle q_e values (not only the final retention percentage), and characterise the spent regenerant for metal concentration and toxicity – data that collectively enable genuine assessment of whether a regenerable biochar system offers a net environmental and economic advantage over single-use activated carbon.

5. Future Research Directions

5.1. Novel Biochar Modification Techniques

Advancements in biochar engineering continue to expand the range of functional modifications aimed at improving heavy metal remediation efficiency across varied wastewater compositions. Researchers are increasingly adopting hybrid approaches that merge traditional activation techniques with targeted chemical or structural alterations, with emphasis on producing multifunctional sorbents capable of simultaneous physical adsorption, chemical complexation, and catalytic transformation. Building from the modification strategies previously described, new techniques focus on introducing specific active sites, controlled pore architectures, and tailored electronic properties to match the binding requirements of different contaminant species. One promising trajectory involves precision heteroatom doping. Nitrogen doping via precursors such as melamine or urea during pyrolysis creates electron-rich domains in the carbon matrix that facilitate coordinate covalent bonding with transition metals [45]. These sites interact not only through electrostatic pathways but also by modulating surface energy to enhance metal ion accessibility in competitive solution environments. Sulphur doping, achieved through incorporation of thiol-bearing compounds before pyrolysis, produces soft donor atoms capable of forming strong affinities with soft acid cations like Hg, distinguishing these surfaces from oxygen-anchored pristine biochars [46]. In mixed-metal effluents, this specific selectivity can radically alter uptake hierarchies. In parallel, advanced impregnation methods have evolved to introduce catalytically active phases directly

 doi:10.20944/preprints202605.1519.v1

within the carbon framework. Metal and metal oxide incorporation is widely reported, iron oxides (FeO, FeOOH) bring not only magnetic recoverability but also redox capabilities to transform toxic ions into less mobile species before immobilization [32].

Manganese oxide-modified chars extend this oxidation capacity while maintaining diverse valence states that can interact with multiple ionic species. More recently, co-doping systems combining nitrogen heteroatoms with dispersed nano-FeO particles have shown synergistic effects, nitrogen groups anchor metals via coordination while iron oxide domains catalyze oxidation-reduction reactions beneficial for contaminants like Cr^{6+}. Emerging physical activation protocols push beyond conventional steam or CO processes. Microwave-assisted activation offers rapid volumetric heating and can be combined with chemical agents for simultaneous etching and functionalization. The localized energy delivery of microwave irradiation promotes uniform pore formation while minimizing structural collapse common in prolonged thermal treatments. This approach is especially valuable when activating magnetic-loaded chars where phase preservation beneath high internal heat is critical for maintaining separation performance post-treatment. Composite biochar development expands operational flexibility by embedding additional sorbent phases into the carbon framework. Clay-biochar composites leverage layered silicate structures for intercalating heavy metals alongside organics [4].

Biochar–zeolite hybrids combine microporous crystal lattices with macro-porous char host networks, enabling staged adsorption: larger organics trapped in char macropores while metals enter zeolite cages. Similarly, graphene-modified biochars employ conductive sheets anchored onto biochar backbones to facilitate electron transfer under AOP conditions, enhancing radical-mediated dismantling of metal-organic complexes. Acid-base surface modulation remains a cornerstone but has been refined through multi-step sequences. For example, acid etching followed by alkaline impregnation allows sequential enhancement: first introducing carboxyl functionalities to strengthen cation complexation [46], then loading alkali elements to create localized high-pH microenvironments favorable for in-situ precipitation of certain metals as hydroxides. The resulting dual-functional surfaces exhibit improved resilience against competing solutes compared with monofunctional counterparts. Novel biological-assisted modification techniques are also gaining traction. Immobilizing specific microbial enzymes or whole cells on biochar surfaces can create bio-reactive adsorbents capable of transforming bound metals into less toxic metabolic products [45]. Post-binding enzymatic reduction of selenium or arsenic species embedded within pores represents one example where biological catalysis complements static adsorption domains. Such biologically modified chars may suit decentralized treatment contexts where low-energy operation and long contact times are feasible. Research into selective ligand grafting introduces another dimension, the covalent attachment of synthetic molecules designed to chelate targeted metals tightly even under fluctuating pH or ionic strengths. Amino-functionalized silanes, phosphorylated organics, or crown ethers tethered onto activated biochar surfaces deliver precision capture mechanisms similar to ion-imprinted polymers but within a more sustainable biomass-derived matrix. These ligands can be chosen based on their stability within aqueous media and matched directly to binding constants for contaminants prevalent in specific industrial waste streams. Moreover, magnetization processes have shifted from simple post-pyrolysis coating to integrated in-situ formation during biomass carbonization [32]. By impregnating feedstocks with iron salts prior to pyrolysis, Fe-containing crystalline phases form uniformly throughout the developing carbon structure rather than just adhering superficially, a configuration that enhances both mechanical durability and consistent magnetic response across particle populations. Hybrid activation using dual-energy sources, such as coupling ultrasonic cavitation with concurrent microwave heating, has been proposed to accelerate dispersion of modifying agents throughout the carbon matrix while physically dismantling larger lignocellulosic domains for subsequent pore generation [4].

Ultrasonication assists penetration of liquid-phase reagents deep into porous channels; microwaves induce rapid internal heating fostering reaction kinetics otherwise limited by diffusion constraints. Finally, attention is turning toward environmentally benign modification chemistries

 doi:10.20944/preprints202605.1519.v1

that avoid residual reagent toxicity. Green oxidants like peracetic acid or plant-derived polyphenols are investigated for introducing reactive oxygen groups without producing hazardous waste streams during preparation [46]. These approaches answer calls from environmental regulators concerned about lifecycle impacts, ensuring that materials used to purify water do not themselves carry secondary pollution liabilities once deployed at scale. The convergence of these novel modification strategies not only augments raw capacity metrics but fundamentally changes how biochar interacts with complex contaminant matrices, they become multifunctional platforms supporting adsorption, transformation, and ease-of-recovery operations tuned to diverse wastewater [45]. By combining precise chemical tailoring with structural innovations rooted in physical processing advances, next generation modified biochar's aim to meet both regulatory compliance pressures outlined earlier, and field performance demands across increasingly heterogeneous pollutant scenarios [32].

5.2. Scaling Up for Industrial Applications

Transitioning biochar technologies from pilot-scale demonstrations to sustainable industrial-scale operation presents intertwined scientific, engineering, and economic challenges. The material characteristics that drive high heavy metal removal efficiencies in controlled laboratory conditions are not always preserved when production volumes increase, feedstock variability rises, and processing environments change [11]. At larger scales, optimization must take into account the complex interplay between reactor design, feedstock logistics, modification procedures, and downstream integration with existing treatment infrastructures. Factors such as thermal profile uniformity during pyrolysis or hydrothermal carbonization become more difficult to control in reactors handling tons of biomass per batch compared to small bench units. Thermal gradients can affect functional group distribution on biochar surfaces, key sites for cation complexation, which means output from different sections of a large reactor may display inconsistent adsorption capacities [53]. Scaled systems thus require refined heat transfer solutions and potentially modular reactor arrays to balance throughput with material quality. Economic feasibility is intricately linked to industrial raw material supply chains [108]. Feedstock must be sourced in quantities sufficient to sustain continuous production while avoiding competition with food or higher value uses. Agricultural residues, forestry by-products, and biosolid wastes each present distinct logistical considerations: seasonal availability for crop residues demands storage strategies; bulky wood wastes require pre-processing like chipping or grinding; sewage sludges contain variable contaminant profiles requiring pre-treatment before pyrolysis. Implementing reliable procurement and pre-conditioning stages at scale ensures consistent physical and chemical characteristics of the output biochar [131].

Without such consistency, process engineers face fluctuating removal efficiencies that complicate compliance with effluent quality standards. Modification procedures shown to enhance laboratory-scale adsorption must also be adapted for bulk processing. Acid or alkali activation using large reagent volumes increases operational costs and creates additional waste streams requiring neutralization before disposal [4]. Continuous-flow chemical impregnation systems, capable of treating large biochar volumes without excessive reagent use, would help reduce both expense and environmental impact. Similarly, embedding magnetic phases like FeO into biochar matrices during large-scale runs calls for uniform distribution across product batches; uneven impregnation could lead to performance variability in integrated wastewater units where easy post-use recovery is expected [53]. Reactor design affects not only production efficiency but also downstream integration into treatment plants. Batch-based pyrolyzers may produce superior control over activation conditions yet limit throughput; continuous rotary kilns or screw-type systems offer higher production capacity but impose constraints on residence time control critical for pore development [11]. Couple this with the requirement to meet specific sorbent particle size distributions suited for fixed-bed columns or fluidized beds in industrial wastewater facilities: scaling paths must align mechanical outputs with hydraulic demands of installed treatment technology. Integration with

 doi:10.20944/preprints202605.1519.v1

industrial water treatment lines requires careful sequencing of biochar contact stages relative to other processes such as coagulation-flocculation or advanced oxidation [16].

Sequential placement optimizes performance, adsorptive removal may follow oxidation stages that free metals from organic complexes, yet plant retrofits must minimize flow disruption and avoid excessive head loss across packed char beds. Large manufacturing plants often operate at flow rates far exceeding lab simulations; designing adsorber vessels sized for thousands of cubic meters per day demands empirical column data under flow regimes matching actual operations rather than idealized plug-flow scenarios. Scaling-up also forces reconsideration of regeneration methods. Frequent replacement at scale would overwhelm budgets despite low per-kilogram production costs because total volume requirements are immense [131]. Regeneration protocols must work reliably for hundreds of kilograms per cycle without degrading pore architecture or stripping functional groups necessary for selective removal [53]. Techniques such as mild acid washes applied via automated cleaning-in-place (CIP) systems could offer cost-effective operation if tailored to site-specific contaminant mixture; however, reagent consumption rates multiplied by industrial volumes call for reclamation loops recovering used regenerants where possible. Environmental considerations intensify at scale. Dust control measures have become essential, biochar fines generated during bulk handling pose inhalation hazards to workers and contribute airborne particulate emissions if not contained [108]. Closed conveyance systems, baghouse filters on grinding equipment, and palletization before shipping into plant premises mitigate these risks while improving hydraulic performance by reducing clogging from loose fines in packed beds. Pilot-to-field transition benefits from progressive scalability studies, not jumping directly from lab batches to full plant integration but including intermediate deployments at semi-industrial scale with continuous monitoring over extended periods [11].

Such studies validate real-world sorption kinetics under authentic wastewater matrices containing co-contaminants absent in synthetic lab solutions. They also expose maintenance patterns: pressure drops increasing due to fouling in oily wastewater or selective site blockage under high-sulphate conditions can inform adjustment before final scale-up. Process parameters determined optimal in small trials often shift under industrial constraints, for example steam activation dwell times shortened due to throughput pressures may yield lower surface areas unless compensated by increased activation agent concentration [53]. Understanding these trade-offs requires collaborative input between material scientists fine-tuning sorbent properties and process engineers prioritizing efficiency metrics tied to plant economics. Supply-side sustainability remains integral: co-location of biochar production facilities within industrial zones generating suitable biomass wastes reduces transport emissions while creating closed-loop treatment ecosystems where waste transforms directly into remediation media [108]. For instance, paper mill sludge converted onsite into tailored char re-enters the mill's own water treatment circuit, a model aligning cost savings with regulatory compliance while reducing external sourcing uncertainties. The transition thus depends upon bridging gaps between high-performing but small-scale materials science achievements outlined previously and the operational realities of industrial wastewater management infrastructure. Addressing variability in feedstock chemistry, maintaining modification uniformity over large volumes, engineering compatible reactor systems within plant layout constraints, and establishing dependable regeneration cycles are all essential steps toward realizing biochar's potential at an operational scale capable of meeting stringent effluent discharge limits continuously under fluctuating load conditions [11,131].

5.3. Environmental Risk Assessment

5.3.1. Leachability Testing Under Relevant pH and Redox Conditions

Biochar deployed in wastewater treatment systems inevitably contacts a range of pH and redox conditions that differ markedly from the controlled conditions of laboratory adsorption experiments, and these differences govern whether sorbed metals remain immobilized or are remobilized into the

 doi:10.20944/preprints202605.1519.v1

treated effluent or receiving environment. Standard regulatory leachability tests – such as the US EPA Toxicity Characteristic Leaching Procedure (TCLP; pH 4.93 acetate buffer, simulating co-disposal with municipal solid waste) and the Synthetic Precipitation Leaching Procedure (SPLP; pH 4.2–5.0, simulating acid rain infiltration) [145] – provide a baseline assessment of leaching risk but do not capture site-specific chemistry. For biochar used in wastewater treatment, the following complementary test conditions are specifically recommended: (i) pH 3–4 leaching tests to simulate acid regeneration cycles and low-pH industrial influents; (ii) pH 8–10 tests to evaluate alkaline dissolution of mineral-phase-bound metals (particularly carbonates and phosphates that can dissolve under high-pH conditions) [54,74]; and (iii) reducing-condition leaching (Eh ≤ −100 mV, achievable by purging with N_2 or CO_2) to assess remobilization of redox-sensitive species such as Cr^{6+}–Cr^{3+} interconversion, As^{5+}–As^{3+} reduction [75,96], and reductive dissolution of Fe-bound metal phases . Evidence in the literature indicates that metals immobilized primarily through surface precipitation (e.g., Pb^{2+} as pyromorphite or cerussite on phosphate-rich chars) are substantially more vulnerable to acid leaching than metals held via inner-sphere complexation at carboxyl or hydroxyl sites, underscoring that the dominant adsorption mechanism (not merely the quantity adsorbed) determines long-term stability. Reporting of leachability data alongside adsorption capacity in future studies would enable a more complete risk-based evaluation of biochar suitability for field deployment.

5.3.2. Aged Biochar Stability

Virtually all published biochar adsorption studies characterise freshly produced material; however, biochar undergoes progressive abiotic and biotic ageing upon environmental exposure that can substantially alter its surface chemistry, pore structure, and metal-binding behaviour [146,147]. Abiotic ageing mechanisms include oxidation of aromatic carbon surfaces to form additional carboxyl and carbonyl groups (increasing hydrophilicity and cation exchange capacity), hydrolysis of ester and anhydride linkages, and dissolution of labile mineral phases. These changes are broadly beneficial for heavy metal adsorption in the short term, as oxidation increases negative surface charge. However, prolonged oxidation can fragment the porous carbon matrix, reducing specific surface area and mechanical strength, and may release previously immobilized metals as the mineral matrix degrades. Biotic ageing (mediated by microbial colonization of biochar pore networks in situ) can competitively occupy adsorption sites, alter local pH through metabolic activity, and produce organic ligands that form soluble metal complexes, potentially increasing rather than decreasing metal mobility. For regulatory and operational purposes, aged biochar stability should be assessed using accelerated ageing protocols: H_2O_2 oxidation (e.g., 30% H_2O_2 for 24 h) [146,149], as an abiotic surrogate, or incubation in inoculated wastewater for 30–90 days as a biotic surrogate, followed by repeat leachability testing. Studies that report adsorption capacity only on fresh biochar, without any ageing assessment, should be interpreted as providing an upper bound on long-term field performance rather than an operational estimate. This distinction (evidence-based conclusion versus forward-looking assumption) is particularly important when biochar is proposed for use in receiving environments such as constructed wetlands or soil amendment, where long-term metal retention, rather than short-term removal, is the critical endpoint.

5.3.3. Ecotoxicity Screening

Chemical leachability testing establishes whether metals are mobile under given conditions, but it does not establish whether mobile concentrations are biologically harmful – that determination requires ecotoxicity screening. The following tiered ecotoxicity endpoints are recommended as a minimum framework for biochar risk characterization: (i) acute aquatic toxicity using standard organisms such as Daphnia magna (48 h EC_{50}) [150] and Aliivibrio fischeri (15 min bioluminescence inhibition assay, ISO 11348) [151,152], which are sensitive to a broad range of heavy metals at low concentrations and require only small volumes of leachate; (ii) plant phytotoxicity using seed germination and early root elongation assays (e.g., Lepidium sativum or Lactuca sativa, ISO 11269-

 doi:10.20944/preprints202605.1519.v1

1)[153] for biochar intended for agricultural or wetland applications where plant uptake is a relevant exposure pathway [154]; and (iii) soil microbial community activity assays (substrate-induced respiration or enzyme activity panels) for biochar proposed for soil amendment, since microbial community disruption by metal-loaded spent biochar represents an indirect ecological risk pathway not captured by chemical analysis alone. It is important to distinguish clearly between what the existing literature establishes as evidence and what remains forward-looking. Evidence-based conclusions currently supported by published data include biochar reduces dissolved metal concentrations in treated effluent under controlled laboratory conditions; certain modified biochars exhibit lower metal leachability than unmodified counterparts in standard TCLP tests; and co-pyrolysis with metal-contaminated feedstocks can concentrate and stabilize metals relative to the original biomass. Forward-looking suggestions that require further validation before operational adoption include biochar-amended constructed wetlands will reliably prevent long-term metal accumulation in receiving soils; ecotoxicity of biochar leachates is negligible across all feedstock and modification types; and aged biochar in field conditions retains adsorption capacity comparable to freshly produced material. Maintaining this distinction between demonstrated findings and research aspirations is essential for credible risk communication to regulators, operators, and downstream users of biochar-treated water.

6. Conclusion

Biochar emerges as a highly promising material for addressing heavy metal contamination in wastewater, offering a potentially sustainable and cost-competitive alternative (noting that comprehensive LCA and techno-economic analyses across diverse feedstock and scale scenarios remain an area for future work) to conventional sorbents. Its unique combination of high porosity, diverse surface functional groups, and inherent mineral content enables multiple adsorption mechanisms, including complexation, ion exchange, physical sorption, and precipitation. The versatility of biochar is further enhanced through various modification techniques, physical activation, chemical functionalization, and composite formation, that improve adsorption capacity, selectivity, and operational resilience. These modifications allow biochar to effectively target a broad spectrum of contaminants, including heavy metals and organic micropollutants, within complex wastewater matrices.

Integration of biochar with advanced treatment technologies such as advanced oxidation processes and biological systems creates synergistic effects that improve overall removal efficiencies. In AOPs, biochar can act as both an adsorbent and a catalyst, facilitating radical generation and subsequent immobilization of liberated metal ions. When combined with biological treatment, biochar serves as a scaffold for microbial colonization, enabling simultaneous adsorption of metals and biodegradation of organics while mitigating toxicity to microbial communities. These hybrid approaches address challenges posed by mixed contaminant streams and variable wastewater chemistries.

Applications across industrial, municipal, and agricultural wastewater demonstrate biochar's adaptability to diverse effluent characteristics and treatment requirements. Industrial effluents benefit from biochar's capacity to handle high pollutant loads and extreme pH or redox conditions, while municipal systems leverage its ability to remove residual metals and emerging contaminants post-secondary treatment. In agricultural runoff scenarios, biochar intercepts diffuse metal and pesticide pollution, contributing to watershed protection and nutrient management. The selection of feedstock and production parameters plays a critical role in optimizing biochar properties for specific applications, emphasizing the need for context-aware material design.

Operational factors such as pH, temperature, contaminant concentration, and co-existing ions influence removal performance, highlighting the importance of process optimization. Regeneration and reuse of biochar are essential for maintaining long-term functionality and economic viability, with thermal, chemical, physical, and biological methods offering various advantages and

 doi:10.20944/preprints202605.1519.v1

limitations. Careful management of regeneration protocols ensures preservation of active sites and structural integrity, enabling multiple treatment cycles while minimizing waste generation.

Environmental and regulatory considerations must guide biochar deployment to prevent unintended ecological impacts. Potential risks include leaching of inherent contaminants, formation of toxic byproducts during production, and effects on soil and microbial communities. Standardized testing, feedstock screening, and controlled production conditions are necessary to mitigate these hazards. Compliance with stringent discharge standards requires treatment systems capable of consistently reducing heavy metal concentrations to safe levels, often necessitating integration of biochar with complementary technologies.

Future research directions focus on novel modification strategies such as heteroatom doping, advanced impregnation, microwave-assisted activation, and bio-reactive composites that enhance adsorption specificity, catalytic activity, and recovery ease. Scaling up production and application involves overcoming challenges related to feedstock variability, reactor design, process control, and integration with existing treatment infrastructure. Addressing these factors will facilitate the transition from laboratory successes to industrial-scale operations capable of meeting regulatory demands and environmental goals.

Overall, biochar represents a multifaceted solution that aligns environmental sustainability with practical wastewater treatment needs. Its capacity to immobilize heavy metals while accommodating complex contaminant profiles positions it as a valuable component in integrated water management frameworks. Continued innovation in material engineering, process optimization, and system integration will be key to realizing its full potential in safeguarding water quality and public health across diverse settings.

References

1. Gupta S, Sireesha S, Sreedhar I, Patel CM, Anitha KL. Latest trends in heavy metal removal from wastewater by biochar-based sorbents. Journal of Water Process Engineering. 2020 Dec 1; 38:101561. https://doi.org/10.1016/j.jwpe.2020.101561
2. Gope M, Saha R. Removal of heavy metals from industrial effluents by using biochar. In: Intelligent environmental data monitoring for pollution management 2021 Jan 1 (pp. 25-48). Academic Press. https://doi.org/10.1016/B978-0-12-819671-7.00002-6
3. Mathabatha TI, Matheri AN, Belaid M. Peanut shell-derived biochar as a low-cost adsorbent to extract cadmium, chromium, lead, copper, and zinc (heavy metals) from wastewater: circular economy approach. Circular Economy and Sustainability. 2023 Jun;3(2):1045-64. https://doi.org/10.1007/s43615-022-00207-4
4. Aziz KH, Kareem R. Recent advances in water remediation from toxic heavy metals using biochar as a green and efficient adsorbent: a review. Case Studies in Chemical and Environmental Engineering. 2023 Dec 1; 8:100495. https://doi.org/10.1016/j.cscee.2023.100495
5. Aziz KH, Mustafa FS, Hassan MA, Omer KM, Hama S. Biochar as green adsorbents for pharmaceutical pollution in aquatic environments: A review. Desalination. 2024 Aug 19; 583:117725. https://doi.org/10.1016/j.desal.2024.117725
6. Chauhan S, Shafi T, Dubey BK, Chowdhury S. Biochar-mediated removal of pharmaceutical compounds from aqueous matrices via adsorption. Waste Disposal & Sustainable Energy. 2023 Mar;5(1):37-62. https://doi.org/10.1007/s42768-022-00118-y
7. Kulkarni SR, Nighojkar A, Kandasubramanian B. Aqueous adsorption of pharmaceutical pollutants on biochar: a review on physicochemical characteristics, classical sorption models, and advancements in machine learning techniques. Water, Air, & Soil Pollution. 2023 Nov;234(11):684. https://doi.org/10.1007/s11270-023-06696-9
8. Olugbenga OS, Adeleye PG, Oladipupo SB, Adeleye AT, John KI. Biomass-derived biochar in wastewater treatment-a circular economy approach. Waste Management Bulletin. 2024 Mar 1;1(4):1-4. https://doi.org/10.1016/j.wmb.2023.07.007

 doi:10.20944/preprints202605.1519.v1

9. Moureen A, Waqas M, Khan N, Jabeen F, Magazzino C, Jamila N, Beyazli D. Untapped potential of food waste derived biochar for the removal of heavy metals from wastewater. Chemosphere. 2024 May 1; 356:141932. https://doi.org/10.1016/j.chemosphere.2024.141932
10. Ighalo JO, Rangabhashiyam S, Dulta K, Umeh CT, Iwuozor KO, Aniagor CO, Eshiemogie SO, Iwuchukwu FU, Igwegbe CA. Recent advances in hydrochar application for the adsorptive removal of wastewater pollutants. Chemical Engineering Research and Design. 2022 Aug 1; 184:419-56. https://doi.org/10.1016/j.cherd.2022.06.028
11. Khanzada AK, Al-Hazmi HE, Kurniawan TA, Majtacz J, Piechota G, Kumar G, Ezzati P, Saeb MR, Rabiee N, Karimi-Maleh H, Lima EC. Hydrochar as a bio-based adsorbent for heavy metals removal: A review of production processes, adsorption mechanisms, kinetic models, regeneration and reusability. Science of the Total Environment. 2024 Oct 1; 945:173972. https://doi.org/10.1016/j.scitotenv.2024.173972
12. Alghamdi AG, Alasmary Z. Efficient remediation of cadmium-and lead-contaminated water by using Fe-modified date palm waste biochar-based adsorbents. International Journal of Environmental Research and Public Health. 2023 Jan 1;20(1):802. https://doi.org/10.3390/ijerph20010802
13. Ye Q, Li Q, Li X. Removal of heavy metals from wastewater using biochars: adsorption and mechanisms. Environmental Pollutants and Bioavailability. 2022 Dec 31;34(1):385-94. https://doi.org/10.1080/26395940.2022.2120542
14. Biswal BK, Balasubramanian R. Use of biochar as a low-cost adsorbent for removal of heavy metals from water and wastewater: A review. Journal of Environmental Chemical Engineering. 2023 Oct 1;11(5):110986. https://doi.org/10.1016/j.jece.2023.110986
15. Awang NA, Wan Salleh WN, Aziz F, Yusof N, Ismail AF. A review on preparation, surface enhancement and adsorption mechanism of biochar-supported nano zero-valent iron adsorbent for hazardous heavy metals. Journal of Chemical Technology & Biotechnology. 2023 Jan;98(1):22-44. https://doi.org/10.1002/jctb.7182
16. Hussain MK, Khatoon S, Nizami G, Fatma UK, Ali M, Singh B, Quraishi A, Assiri MA, Ahamad S, Saquib M. Unleashing the power of bio-adsorbents: efficient heavy metal removal for sustainable water purification. Journal of Water Process Engineering. 2024 Jul 1; 64:105705. https://doi.org/10.1016/j.jwpe.2024.105705
17. Cairns S, Robertson I, Sigmund G, Street-Perrott A. The removal of lead, copper, zinc and cadmium from aqueous solution by biochar and amended biochars. Environmental Science and Pollution Research. 2020 Jun;27(17):21702-15. https://doi.org/10.1007/s11356-020-08706-3
18. Shukla P, Giri BS, Mishra RK, Pandey A, Chaturvedi P. Lignocellulosic biomass-based engineered biochar composites: a facile strategy for abatement of emerging pollutants and utilization in industrial applications. Renewable and Sustainable Energy Reviews. 2021 Dec 1; 152:111643. https://doi.org/10.1016/j.rser.2021.111643
19. Abiodun OA, Oluwaseun O, Oladayo OK, Abayomi O, George AA, Opatola E, Orah RF, Isukuru EJ, Ede IC, Oluwayomi OT, Okolie JA. Remediation of heavy metals using biomass-based adsorbents: adsorption kinetics and isotherm models. Clean Technologies. 2023 Jul 28;5(3):934-60. https://doi.org/10.3390/cleantechnol5030047
20. Ghosh S, Nandasana M, Webster TJ, Thongmee S. Agrowaste-generated biochar for the sustainable remediation of refractory pollutants. Frontiers in Chemistry. 2023 Nov 16; 11:1266556. https://doi.org/10.3389/fchem.2023.1266556
21. Awogbemi O, Von Kallon DV. Progress in agricultural waste derived biochar as adsorbents for wastewater treatment. Applied Surface Science Advances. 2023 Dec 1; 18:100518. https://doi.org/10.1016/j.apsadv.2023.100518
22. Mariana M, Hps AK, Mistar EM, Yahya EB, Alfatah T, Danish M, Amayreh M. Recent advances in activated carbon modification techniques for enhanced heavy metal adsorption. Journal of Water Process Engineering. 2021 Oct 1; 43:102221. https://doi.org/10.1016/j.jwpe.2021.102221
23. Petrović J, Koprivica M, Ercegović M, Simić M, Dimitrijević J, Bugarčić M, Trifunović S. Synthesis and application of FeMg-modified hydrochar for efficient removal of lead ions from aqueous solution. Processes. 2025 Jun 29;13(7):2060. https://doi.org/10.3390/pr13072060

 doi:10.20944/preprints202605.1519.v1

24. Ercegović M, Petrović J, Koprivica M, Simić M, Dimitrijević J, Trifunović S, Krstić J. Hierarchical microporous miscanthus-derived activated carbon enables entropy-driven high-efficiency dye removal. Green Processing and Synthesis. 2026 Jan 23;15(1):20250165. https://doi.org/10.1515/gps-2025-0165
25. Beljin J, Kragulj Isakovski M, Maletić S. Engineering Multifunctional Biochars for Integrated Environmental Systems: Multi-Medium Performance, Challenges, and Research Priorities. Processes. 2026 Feb 21;14(4):714. https://doi.org/10.3390/pr14040714
26. International Biochar Initiative (IBI). Standardized Product Definition and Product Testing Guidelines for Biochar That Is Used in Soil (IBI Biochar Standards, Version 2.1). International Biochar Initiative; 2015. Available from: https://biochar-international.org/wp-content/uploads/2020/06/IBI_Biochar_Standards_V2.1_Final2.pdf
27. Zuo H, Xia Y, Liu H, Liu Z, Huang Y. Preparation of activated carbon with high nitrogen content from agro-industrial waste for efficient treatment of chromium (VI) in water. Industrial Crops and Products. 2023 Apr 1; 194:116403. https://doi.org/10.1016/j.indcrop.2023.116403
28. Nazbakhsh M, Nabavi SR, Jafarian S. Optimized production of high-performance activated biochar from sugarcane bagasse via systematic pyrolysis and chemical activation. Sustainability. 2025 Feb 13;17(4):1554. https://doi.org/10.3390/su17041554
29. Mu J, Chen Y, Wu X, Chen Q, Zhang M. Rapid and efficient removal of multiple heavy metals from diverse types of water using magnetic biochars derived from antibiotic fermentation residue. Journal of environmental management. 2024 Feb 1; 351:119685. https://doi.org/10.1016/j.jenvman.2023.119685
30. Haider MI, Liu G, Yousaf B, Arif M, Aziz K, Ashraf A, Safeer R, Ijaz S, Pikon K. Synergistic interactions and reaction mechanisms of biochar surface functionalities in antibiotics removal from industrial wastewater. Environmental Pollution. 2024 Sep 1; 356:124365. https://doi.org/10.1016/j.envpol.2024.124365
31. Gupta P, Gupta N. Potential role of biochar in water treatment. Desalination and Water Treatment. 2022 Mar 1; 251:79–104. https://doi.org/10.5004/dwt.2022.27976
32. Hama Aziz KH, Fatah NM, Muhammad KT. Advancements in application of modified biochar as a green and low-cost adsorbent for wastewater remediation from organic dyes. Royal Society Open Science. 2024 May 15;11(5):232033. https://doi.org/10.1098/rsos.232033
33. Mohan D, Sarswat A, Ok YS, Pittman Jr CU. Organic and inorganic contaminants removal from water with biochar, a renewable, low cost and sustainable adsorbent–a critical review. Bioresource technology. 2014 May 1; 160:191–202. https://doi.org/10.1016/j.biortech.2014.01.120
34. Tran HN, You SJ, Chao HP. Effect of pyrolysis temperatures and times on the adsorption of cadmium onto orange peel derived biochar. Waste Management & Research. 2016 Feb;34(2):129-38. https://doi.org/10.1177/0734242X15615698
35. Peng H, Gao P, Chu G, Pan B, Peng J, Xing B. Enhanced adsorption of Cu (II) and Cd (II) by phosphoric acid-modified biochars. Environmental Pollution. 2017 Oct 1; 229:846-53. https://doi.org/10.1016/j.envpol.2017.07.004
36. Tan X, Liu Y, Zeng G, Wang X, Hu X, Gu Y, Yang Z. Application of biochar for the removal of pollutants from aqueous solutions. Chemosphere. 2015 Apr 1; 125:70-85. https://doi.org/10.1016/j.chemosphere.2014.12.058
37. Prapagdee S, Piyatiratitivorakul S, Petsom A. Physico-chemical activation on rice husk biochar for enhancing of cadmium removal from aqueous solution. Asian Journal of Water, Environment and Pollution. 2016 Jan 19;13(1):27-34. https://doi.org/10.3233/AJW-160004
38. Frolova L, Kharytonov M, Klimkina I, Kovrov O, Koveria A. Investigation of the adsorption of ions chromium by mean biochar from coniferous trees. Applied Nanoscience. 2022 Apr;12(4):1123-9.https://doi.org/10.1007/s13204-021-01995-1
39. Arán DS, Deza M, Monferrán MV, Pignata ML, Harguinteguy CA. Use of local waste for biochar production: Influence of feedstock and pyrolysis temperature on chromium removal from aqueous solutions. Integrated Environmental Assessment and Management. 2023 May 1;19(3):717-25. https://doi.org/10.1002/ieam.4643

 doi:10.20944/preprints202605.1519.v1

40. Uchimiya M, Wartelle LH, Klasson KT, Fortier CA, Lima IM. Influence of pyrolysis temperature on biochar property and function as a heavy metal sorbent in soil. Journal of agricultural and food chemistry. 2011 Mar 23;59(6):2501-10. https://doi.org/10.1021/jf104206c
41. Sun T, Aslam MMA, Chen G, Ye Y, Xu W, Peng C. Properties of biochar prepared by solar pyrolysis and its adsorption of Cu^{2+} in water. Earth Sci. 2024;13(4):151–162. https://doi.org/10.11648/j.earth.20241304.14
42. Inyang MI, Gao B, Yao Y, Xue Y, Zimmerman A, Mosa A, Pullammanappallil P, Ok YS, Cao X. A review of biochar as a low-cost adsorbent for aqueous heavy metal removal. Critical reviews in environmental science and technology. 2016 Feb 16;46(4):406-33. https://doi.org/10.1080/10643389.2015.1096880
43. Lu T, Yuan H, Wang Y, Huang H, Chen Y. Characteristic of heavy metals in biochar derived from sewage sludge. Journal of Material Cycles and Waste Management. 2016 Sep;18(4):725-33. https://doi.org/10.1007/s10163-015-0366-y
44. Chen T, Zhang Y, Wang H, Lu W, Zhou Z, Zhang Y, Ren L. Influence of pyrolysis temperature on characteristics and heavy metal adsorptive performance of biochar derived from municipal sewage sludge. Bioresource technology. 2014 Jul 1; 164:47-54. https://doi.org/10.1016/j.biortech.2014.04.048
45. Zhang J, Chen Z, Liu Y, Wei W, Ni BJ. Removal of emerging contaminants (ECs) from aqueous solutions by modified biochar: a review. Chemical Engineering Journal. 2024 Jan 1; 479:147615. https://doi.org/10.1016/j.cej.2023.147615
46. Boraah N, Chakma S, Kaushal P. Attributes of wood biochar as an efficient adsorbent for remediating heavy metals and emerging contaminants from water: a critical review and bibliometric analysis. Journal of Environmental Chemical Engineering. 2022 Jun 1;10(3):107825. https://doi.org/10.1016/j.jece.2022.107825
47. Zhou X, Yang Y, Yang R, Shi L, Zhou L, Lv X. Preparation of chitosan-EDTA bifunctionally modified magnetic walnut shell biochar and study on its copper ion (Cu (ii)) adsorption performance. RSC advances. 2026;16(4):3220-30. https://doi.org/10.1039/d5ra08820h
48. Qin H, Shao X, Shaghaleh H, Gao W, Hamoud YA. Adsorption of Pb2+ and Cd2+ in agricultural water by potassium permanganate and nitric acid-modified coconut shell biochar. Agronomy. 2023 Jul 7;13(7):1813. https://doi.org/10.3390/agronomy13071813
49. Brunauer S, Emmett PH, Teller E. Adsorption of gases in multimolecular layers. Journal of the American Chemical Society. 1938;60(2):309–19. https://doi.org/10.1021/ja01269a023
50. Lowell S, Shields JE, Thomas MA, Thommes M. Characterization of porous solids and powders: surface area, pore size and density. Springer Science & Business Media; 2012 Sep 14. https://doi.org/10.1007/978-1-4020-2303-3
51. Sing KS. Reporting physisorption data for gas/solid systems with special reference to the determination of surface area and porosity (Recommendations 1984). Pure and applied chemistry. 1985 Jan 1;57(4):603-19. https://doi.org/10.1351/pac198557040603
52. Rouquerol J, Rouquerol F, Llewellyn P, Maurin G, Sing K. Adsorption by powders and porous solids: principles, methodology and applications. Academic press; 2013 Sep 6.
53. Fseha YH, Shaheen JF, Sizirici B. Revealing selected groundwater contaminants, risks, and sustainable solutions for safe drinking water through pristine and modified biochar. Journal of Analytical and Applied Pyrolysis. 2023 Nov 1; 176:106237. https://doi.org/10.1016/j.jaap.2023.106237
54. Liu C, Lin J, Chen H, Wang W, Yang Y. Comparative study of biochar modified with different functional groups for efficient removal of Pb (II) and Ni (II). International Journal of Environmental Research and Public Health. 2022 Sep 6;19(18):11163. https://doi.org/10.3390/ijerph191811163
55. Qiu B, Tao X, Wang H, Li W, Ding X, Chu H. Biochar as a low-cost adsorbent for aqueous heavy metal removal: A review. Journal of Analytical and Applied Pyrolysis. 2021 May 1; 155:105081. https://doi.org/10.1016/j.jaap.2021.105081
56. Amusat SO, Kebede TG, Dube S, Nindi MM. Ball-milling synthesis of biochar and biochar–based nanocomposites and prospects for removal of emerging contaminants: A review. Journal of Water Process Engineering. 2021 Jun 1; 41:101993. https://doi.org/10.1016/j.jwpe.2021.101993
57. Akhtar MS, Ali S, Zaman W. Innovative adsorbents for pollutant removal: exploring the latest research and applications. Molecules. 2024 Sep 11;29(18):4317. https://doi.org/10.3390/molecules29184317

 doi:10.20944/preprints202605.1519.v1

58. Han L, Qian L, Liu R, Chen M, Yan J, Hu Q. Lead adsorption by biochar under the elevated competition of cadmium and aluminium. Scientific Reports. 2017 May 23;7(1):2264. https://doi.org/10.1038/s41598-017-02353-4
59. Cui L, Yan J, Li L, Quan G, Ding C, Chen T, Yin C, Gao J, Hussain Q. Does biochar alter the speciation of Cd and Pb in aqueous solution? BioResources. 2015;10(1):88–104. https://doi.org/10.15376/BIORES.10.1.88-104
60. Wang Y, Zeng X, Li Q, Jin J, Xiao S, Xu X, Ding W. Surface Functionalizing Woody Biochar with UV Irradiation to Promote Adsorption of Heavy Metals. BioResources. 2024 Oct 1;19(4). https://doi.org/10.15376/biores.19.4.7566-7590
61. Rabiee Abyaneh M, Nabi Bidhendi G, Daryabeigi Zand A. Pb (II), Cd (II), and Mn (II) adsorption onto pruning-derived biochar: physicochemical characterization, modelling and application in real landfill leachate. Scientific Reports. 2024 Feb 10;14(1):3426. https://doi.org/10.1038/s41598-024-54028-6
62. Fahmi AH, Jol H, Singh D. Physical modification of biochar to expose the inner pores and their functional groups to enhance lead adsorption. RSC advances. 2018;8(67):38270-80. https://doi.org/10.1039/c8ra06867d
63. Cui LiQiang CL, Chen TianMing CT, Yin ChunTao YC, Yan JinLong YJ, Ippolito JA, Hussain Q. Mechanism of adsorption of cadmium and lead ions by iron-activated biochar.2019. https://doi.org/10.15376/BIORES.14.1.842-857
64. Peng S, Liu J, Pan G, Qin Y, Yang Z, Yang X, Gu M, Zhu Z, Wei Y. Combining SiO2 NPs with biochar: a novel composite for enhanced cadmium removal from wastewater and alleviation of soil cadmium stress. Environmental Geochemistry and Health. 2024 Nov;46(11):456. https://doi.org/10.1007/s10653-024-02243-5
65. Lin F, Zeng J, Chen J, Li S, Lin W. Treatment of cadmium and lead ions from aqueous media and battery factory wastewater using a magnetic carboxymethyl cellulose/tea waste biochar/$CoFe_2O4$/ZIF-67 composite bioaerogel. International Journal of Biological Macromolecules. 2025 Aug 22:147071. https://doi.org/10.1016/j.ijbiomac.2025.138164
66. Mei Y, Zhuang S, Wang J. Adsorption of heavy metals by biochar in aqueous solution: A review. Science of The Total Environment. 2025 Mar 10; 968:178898. https://doi.org/10.1016/j.scitotenv.2025.178898
67. Ahuja R, Kalia A, Sikka R, P C. Nano modifications of biochar to enhance heavy metal adsorption from wastewaters: a review. ACS omega. 2022 Dec 9;7(50):45825-36. https://doi.org/10.1021/acsomega.2c05117
68. Rafiq S, Wongrod S, Vinitnantharat S. Adsorption kinetics of cadmium and lead by biochars in single-and bisolute brackish water systems. ACS omega. 2023 Nov 20;8(48):45262-76. https://doi.org/10.1021/acsomega.3c03335
69. Titikshya S, Sahoo M, Tyagi I, Naik SN, Kumar V. Production of rhododendron and marigold waste derived biochar: a sustainable innovation to reduce environmental stress. Environment, Development and Sustainability. 2024 Jun 20:1-20. https://doi.org/10.1007/s10668-024-05061-y
70. Ambaye TG, Vaccari M, van Hullebusch ED, Amrane A, Rtimi SJ. Mechanisms and adsorption capacities of biochar for the removal of organic and inorganic pollutants from industrial wastewater. International Journal of Environmental Science and Technology. 2021 Oct;18(10):3273-94. https://doi.org/10.1007/s13762-020-03060-w
71. Wang Y, Chen L, Zhu Y, Fang W, Tan Y, He Z, Liao H. Research status, trends, and mechanisms of biochar adsorption for wastewater treatment: a scientometric review. Environmental Sciences Europe. 2024 Feb 12;36(1):25. https://doi.org/10.1186/s12302-024-00859-z
72. Chen WH, Hoang AT, Nižetić S, Pandey A, Cheng CK, Luque R, Ong HC, Thomas S, Nguyen XP. Biomass-derived biochar: From production to application in removing heavy metal-contaminated water. Process Safety and Environmental Protection. 2022 Apr 1; 160:704-33. https://doi.org/10.1016/j.psep.2022.02.061
73. Lohan D, Jain R, Srivastava A, Dutta S, Mohan D, Sharma RK. Surface engineering approaches for the design of magnetic biochar-composites for removal of heavy metals: A comprehensive review. Journal of Environmental Chemical Engineering. 2023 Dec 1;11(6):111448. https://doi.org/10.1016/j.jece.2023.111448
74. Noreen S, Abd-Elsalam KA. Biochar-based nanocomposites: A sustainable tool in wastewater bioremediation. InAquananotechnology 2021 Jan 1 (pp. 185-200). Elsevier. https://doi.org/10.1016/B978-0-12-821141-0.00023-9

 doi:10.20944/preprints202605.1519.v1

75. Gholizadeh M, Hu X. Removal of heavy metals from soil with biochar composite: A critical review of the mechanism. Journal of Environmental Chemical Engineering. 2021 Oct 1;9(5):105830. https://doi.org/10.1016/j.jece.2021.105830
76. Chen Q, Wang Y, He G, Yilmaz M, Yuan S. KMnO4-activated spinach waste biochar: An efficient adsorbent for adsorption of heavy metal ions in aqueous solution. Colloids and Surfaces A: Physicochemical and Engineering Aspects. 2024 Mar 5; 684:133174. https://doi.org/10.1016/j.colsurfa.2024.133174
77. Oguntimein GB. Biosorption of heavy metals, dyes and contaminants emerging of concern by lignocellulosic biomass. Chemical Science and Chemical Engineering. 2020. [DOI to be verified — previously listed DOI 10.1021/ja02242a004 belongs to Langmuir 1918 and is incorrect]
78. Langmuir I. The adsorption of gases on plane surfaces of glass, mica and platinum. Journal of the American Chemical society. 1918 Sep;40(9):1361-403. https://doi.org/10.1021/ja02242a004
79. Oguntimein GB. Biosorption of heavy metals, dyes and contaminants emerging of concern by lignocellulosic biomass. Chemical Science and Chemical Engineering. 2020.
80. Freundlich H. Über die adsorption in lösungen. Zeitschrift für physikalische Chemie. 1907 Oct 1;57(1):385-470.
81. Lagergren S. About the theory of so-called adsorption of solution substances. Kungliga Svenska Vetenskapsakademiens Handlingar. 1898;24(4):1–39.
82. Ho YS, McKay G. Pseudo-second order model for sorption processes. Process biochemistry. 1999 Jul 1;34(5):451-65. https://doi.org/10.1016/S0032-9592(98)00112-5
83. Wang S, Li X, Zhu Y. Comparison of the adsorption capacity and mechanisms of mixed heavy metals in wastewater by sheep manure biochar and Robinia pseudoacacia biochar. Water Science & Technology. 2023 Jun 15;87(12):3083-94. https://doi.org/10.2166/wst.2023.180
84. Yong SK, Amin S, Tay CC, Rashid NF, Kassim NQ, Siging V. Sorption of Lead from Aqueous System using Palm Kernel Shell Biochar: Kinetic and Isotherm Studies. https://doi.org/10.55373/mjchem.v25i2.117
85. Poonam, Bharti, S. K., and Kumar, N. (2018). Kinetic study of lead (Pb2+) removal from battery manufacturing wastewater using bagasse biochar as biosorbent. Applied Water Science, 8(4), 119. https://doi.org/10.1007/s13201-018-0765-z
86. Zand AD, Abyaneh MR. Adsorption of Lead, manganese, and copper onto biochar in landfill leachate: implication of non-linear regression analysis. Sustainable Environment Research. 2020 Sep 9;30(1):18. https://doi.org/10.21203/rs.3.rs-26558/v1
87. Fu W, Li M, Chen H, Qu J, Zhang L, Qiu S, Feng M, Yuan M, Guo C, Zhou J, Du Z. Novel utilization exploration for the dephosphorization waste of Ca–modified biochar: enhanced removal of heavy metal ions from water. Biochar. 2024 Sep 11;6(1):77. https://doi.org/10.1007/s42773-024-00373-8
88. Choudhary V, Patel M, Pittman Jr CU, Mohan D. Batch and continuous fixed-bed lead removal using himalayan pine needle biochar: isotherm and kinetic studies. ACS omega. 2020 Jul 2;5(27):16366-78. https://doi.org/10.1021/acsomega.0c00216
89. Mo G, Xiao J, Gao X. To enhance the Cd^{2+} adsorption capacity on coconut shell-derived biochar by chitosan modifying: performance and mechanism. Biomass Conversion and Biorefinery. 2023 Dec;13(18):16737-52. https://doi.org/10.1007/s13399-021-02155-9
90. Tho PT, Van HT, Nguyen LH, Hoang TK, Tran TN, Nguyen TT, Nguyen TB, Nguyen VQ, Le Sy H, Thai VN, Tran QB. Enhanced simultaneous adsorption of As (iii), Cd (ii), Pb (ii) and Cr (vi) ions from aqueous solution using cassava root husk-derived biochar loaded with ZnO nanoparticles. RSC advances. 2021;11(31):18881-97. https://doi.org/10.1039/d1ra01599k
91. Li T, Wang Y, Niu Y, Zhang Z, Liu J, Wang X, Wang J, Li J, Wang L. Enhanced Cadmium Adsorption Mechanisms Utilizing Biochar Derived from Different Parts of Wetland Emergent Plants Iris sibirica L. Processes. 2025 May 15;13(5):1520. https://doi.org/10.3390/pr13051520
92. Dad FP, Sharif F, Nizami AS. Adsorption of trace heavy metals through organic compounds enriched biochar using isotherm adsorption and kinetic models. Environmental research. 2024 Jan 15; 241:117702. https://doi.org/10.1016/j.envres.2023.117702
93. Zhou R, Zhang M, Shao S. Optimization of target biochar for the adsorption of target heavy metal ion. Scientific reports. 2022 Aug 11;12(1):13662. https://doi.org/10.1038/s41598-022-17901-w

 doi:10.20944/preprints202605.1519.v1

94. Vidhya L, Ramya T, Vinodha S. Mesoporous biochar obtained from coir pith on removing nickel (II) from aqueous simulated solution–batch and column studies. Desalination and Water Treatment. 2020 Dec 1; 206:202-14. https://doi.org/10.5004/dwt.2020.26265
95. Yang L, He L, Xue J, Wu L, Ma Y, Li H, Peng P, Li M, Zhang Z. Highly efficient nickel (II) removal by sewage sludge biochar supported α-Fe2O3 and α-FeOOH: Sorption characteristics and mechanisms. PLoS One. 2019 Jun 12;14(6): e0218114. https://doi.org/10.1371/journal.pone.0218114
96. Hu W, Zhang X, Chen M, Rahman ST, Li X, Wang G. Enhancing Cr (VI) adsorption of chestnut shell biochar through H3PO4 activation and nickel doping. Molecules. 2024 May 9;29(10):2220. https://doi.org/10.3390/molecules29102220
97. Cui X, Wang J, Zhao Q, Li C, Huang J, Hu X, Li J, Li M. Application of a novel bifunctionalized magnetic biochar to remove Cr (VI) from wastewater: performance and mechanism. Separations. 2023 Jun 15;10(6):358. https://doi.org/10.3390/separations10060358
98. Murtaza G, Usman M, Ahmed Z, Rizwan M, Iqbal R. Non-wood-based biochars as promising and eco-friendly adsorbents for chromium hexavalent Cr (VI) removal from aquatic systems: state-of-the-art, limitations, and potential future directions. Environmental Pollutants and Bioavailability. 2024 Dec 31;36(1):2387680. https://doi.org/10.1080/26395940.2024.2387680
99. Wilson K, Iqbal J, Obaid Abdalla Obaid Hableel A, Naji Khalaf Beyaha Alzaabi Z, Nazzal Y. Camel dung-derived biochar for the removal of Copper (II) and Chromium (III) Ions from aqueous solutions: adsorption and kinetics studies. ACS omega. 2024 Feb 27;9(10):11500-9. https://doi.org/10.1021/acsomega.3c08230
100. Hamadneh I, Jukhan MA, Damer K, Alkhaza'leh H, Hammad H, Qanadilo S, Al-Dujaili AH. Preparation and Adsorption Properties of Biochar Derived from Biomass of Jacaranda mimosifolia Fruit Pod for the Removal of Cr (VI) Ion from Aqueous Solution. Water, Air, & Soil Pollution. 2026 Jan;237(2):70. https://doi.org/10.1007/s11270-025-08785-3
101. Ashfaq-Butt T. Efficient Removal of Hexavalent Chromium with Novel Agro-Waste Biochar. Croatica Chemica Acta. 2025 Feb 2;98(1):P1-5. https://doi.org/10.5562/cca4096
102. Kurniawan TA, Ali S, Mohyuddin A, Haider A, Riaz M, Khan S, Othman MH, Goh HH, Anouzla A, Aziz F, Ali I. Cultivating sustainability: Harnessing biochar-derived composites for carbon-neutral wastewater treatment. Process Safety and Environmental Protection. 2024 Jul 1; 187:665-97.https://doi.org/10.1016/j.psep.2024.04.040
103. Kearns J, Dickenson E, Aung MT, Joseph SM, Summers SR, Knappe D. Biochar water treatment for control of organic micropollutants with UVA surrogate monitoring. Environmental Engineering Science. 2021 May 1;38(5):298-309. https://doi.org/10.1089/ees.2020.0173
104. Fseha, Y. H., Sizirici, B., Yildiz, I., and Yavuz, C. (2022). Pristine biochar performance investigation to remove metals in primary and secondary treated municipal wastewater for groundwater recharge application. PloS one, 17(12), e0278315. https://doi.org/10.1371/journal.pone.0278315
105. Mahmoud AE, Kathi S. Assessment of biochar application in decontamination of water and wastewater. InCost effective technologies for solid waste and wastewater treatment 2022 Jan 1 (pp. 69-74). Elsevier. https://doi.org/10.1016/B978-0-12-822933-0.00009-7
106. Li C, Zhang C, Zhong S, Duan J, Li M, Shi Y. The removal of pollutants from wastewater using magnetic biochar: a scientometric and visualization analysis. Molecules. 2023 Aug 3;28(15):5840. https://doi.org/10.3390/molecules28155840
107. Padhi P, Bora N, Sohtun P, Athparia M, Kumar M, Kataki R, Sarangi PK. Remediation of mine overburden and contaminated water with activated biochar derived from low-value biowaste. Journal of the Taiwan Institute of Chemical Engineers. 2024 Jun 1;159:105472. https://doi.org/10.1016/j.jtice.2024.105472
108. Nworie FS, Mgbemena N, Ike-Amadi AC, Ebunoha J. Functionalized biochars for enhanced removal of heavy metals from aqueous solutions: mechanism and future industrial prospects. Journal of Human, Earth, and Future. 2022 Sep;3(3):377-95. http://dx.doi.org/10.28991/HEF-2022-03-03-09
109. Zeghioud H, Fryda L, Djelal H, Assadi A, Kane A. A comprehensive review of biochar in removal of organic pollutants from wastewater: Characterization, toxicity, activation/functionalization and influencing treatment factors. Journal of Water Process Engineering. 2022 Jun 1; 47:102801. https://doi.org/10.1016/j.jwpe.2022.102801

 doi:10.20944/preprints202605.1519.v1

110. Koprivica M, Simić M, Petrović J, Ercegović M, Dimitrijević J. Evaluation of adsorption efficiency on Pb (II) ions removal using Alkali-modified hydrochar from paulownia leaves. Processes. 2023 Apr 25;11(5):1327. https://doi.org/10.3390/pr11051327
111. Ungureanu G, Bejenari I, Hristea G, Volf I. Carbonaceous materials from forest waste conversion and their corresponding hazardous pollutants remediation performance. Forests. 2022 Dec 7;13(12):2080. https://doi.org/10.3390/f13122080
112. Nakić D, Posavčić H, Matošević D, Tomaš I. perspectives on the application of biochar produced from sewage sludge gasification in wastewater treatment for heavy metals removal. Environmental Engineering-Inženjerstvo okoliša. 2025 Dec 18;12(1-2):26-34. https://doi.org/10.37023/ee.12.1-2.3
113. Bożęcka A, Orlof-Naturalna M, Sanak-Rydlewska S. Removal of lead, cadmium and copper ions from aqueous solutions by using ion exchange resin C 160. Gospodarka Surowcami Mineralnymi. 2016;32(4):129-39. https://doi.org/10.1515/gospo-2016-0033
114. Pam AA, Abdullah AH, Ping TY, Zainal Z. Batch and fixed bed adsorption of Pb (II) from aqueous solution using EDTA modified activated carbon derived from palm kernel shell. BioResources. 2018 Jan 1;13(1):1235-50. https://doi.org/10.15376/biores.13.1.1235-1250
115. Guo X, Liu A, Lu J, Niu X, Jiang M, Ma Y, Liu X, Li M. Adsorption mechanism of hexavalent chromium on biochar: kinetic, thermodynamic, and characterization studies. ACS omega. 2020 Oct 19;5(42):27323-31. https://doi.org/10.1021/acsomega.0c03652
116. Li Y, Peng L, Li W. Adsorption behaviours on trace Pb2+ from water of biochar adsorbents from konjac starch. Adsorption Science & Technology. 2020 Dec;38(9-10):344-56. https://doi.org/10.1177/0263617420948699
117. Jia Y, Zhang Y, Fu J, Yuan L, Li Z, Liu C, Zhao D, Wang X. A novel magnetic biochar/MgFe-layered double hydroxides composite removing Pb2+ from aqueous solution: Isotherms, kinetics and thermodynamics. Colloids and Surfaces A: Physicochemical and Engineering Aspects. 2019 Apr 20; 567:278-87.https://doi.org/10.1016/j.colsurfa.2019.01.064
118. Saha M, Biswas PK, Saha JK, Sarkar A, Mandal S, Yadav DK, Lenka S, Coumar MV, Basak BB. Synthesis of nitrogen-purged biochar and modification with hydrothermal activation: comparative assessment as adsorbents for effective elimination of Pb (II) and Cd (II) from wastewater. Discover Applied Sciences. 2025 Feb;7(2):1-9. https://doi.org/10.1007/s42452-025-06589-y
119. Ge S, Zhao S, Wang L, Zhao Z, Wang S, Tian C. Exploring adsorption capacity and mechanisms involved in cadmium removal from aqueous solutions by biochar derived from euhalophyte. Scientific Reports. 2024 Jan 3;14(1):450. https://doi.org/10.1038/s41598-023-50525-2
120. Štefelová J, Zelenka T, Slovák V. Biosorption (removing) of Cd (II), Cu (II) and methylene blue using biochar produced by different pyrolysis conditions of beech and spruce sawdust. Wood Science and Technology. 2017 Nov;51(6):1321-38. https://doi.org/10.1007/s00226-017-0928-3
121. Li Y, Zhao B, Shang T. Adsorption of copper (II) in biochar-humic acid–water system. Scientific Reports. 2025 Jul 10;15(1):24948. https://doi.org/10.1038/s41598-025-09880-5
122. Zhang H, Xiao R, Li R, Ali A, Chen A, Zhang Z. Enhanced aqueous Cr (VI) removal using chitosan-modified magnetic biochars derived from bamboo residues. Chemosphere. 2020 Dec 1; 261:127694. https://doi.org/10.1016/j.chemosphere.2020.127694
123. Azadian M, Gilani HG. Adsorption of Cu2+, Cd2+, and Zn2+ by engineered biochar: Preparation, characterization, and adsorption properties. Environmental Progress & Sustainable Energy. 2023 Jul;42(4):e14088. https://doi.org/10.1002/ep.14088
124. Alam MS, Gorman-Lewis D, Chen N, Flynn SL, Ok YS, Konhauser KO, Alessi DS. Thermodynamic analysis of nickel (II) and zinc (II) adsorption to biochar. Environmental science & technology. 2018 May 10;52(11):6246-55. https://doi.org/10.1021/acs.est.7b06261
125. Han Z, Guo Z, Zhang Y, Xiao X, Xu Z, Sun Y. Pyrolysis characteristics of biomass impregnated with cadmium, copper and lead: influence and distribution. Waste and Biomass Valorization. 2018 Jul;9(7):1223-30. https://doi.org/10.1007/s12649-017-0036-5

 doi:10.20944/preprints202605.1519.v1

126. Masud MAI, Ye Z, Papadopoulos V, Langford J, Yee LH, Morel M, Naidu R. Iron biochar synergy in aquatic systems through surface functionalities, electron transfer and reactive species dynamics. npj Clean Water. 2025;8(1):61. https://doi.org/10.1038/s41545-025-00471-5
127. Badiger SM, Nidheesh PV. Applications of biochar in sulphate radical-based advanced oxidation processes for the removal of pharmaceuticals and personal care products. Water Science & Technology. 2023 Mar 15;87(6):1329-48. https://doi.org/10.2166/wst.2023.069
128. Xu S, Liang M, Ding Y, Wang D, Zhu Y, Han L. Synthesis, optical characterization, and adsorption of novel hexavalent chromium and total chromium sorbent: a fabrication of mulberry stem biochar/Mn-Fe binary oxide composite via response surface methodology. Frontiers in Environmental Chemistry. 2021 Aug 10;2:692810. https://doi.org/10.3389/fenvc.2021.692810
129. Yang Z, Wang J, Zhao N, Tang X, Shi T, Zheng Z, Bao M, Liu Y, Chen X. A novel biochar-based 3D composite for ultrafast and selective Cr^{6+} removal in electroplating wastewater. Biochar. 2024; 6:46. https://doi.org/10.1007/s42773-024-00338-x
130. Martiny TR, Avila LB, Rodrigues TL, Tholozan LV, Meili L, de Almeida AR, da Rosa GS. From waste to wealth: Exploring biochar's role in environmental remediation and resource optimization. Journal of Cleaner Production. 2024 May 10; 453:142237. https://doi.org/10.1016/j.jclepro.2024.142237
131. Kumkum P, Kumar S. A review on biochar as an adsorbent for Pb (II) removal from water. Biomass. 2024 Apr 2;4(2):243-72. https://doi.org/10.3390/biomass4020012
132. Alsawy T, Rashad E, El-Qelish M, Mohammed RH. A comprehensive review on the chemical regeneration of biochar adsorbent for sustainable wastewater treatment. NPJ Clean Water. 2022 Jul 11;5(1):29. https://doi.org/10.1038/s41545-022-00172-3
133. Wu Y, Wang Z, Yan Y, Zhou Y, Huma B, Tan Z, Zhou T. Recovery and regeneration of water-hardened magnetic composite biochar sphere for the removal of multiple heavy metals in contaminated soils. Journal of Cleaner Production. 2024 Apr 15; 450:141906. https://doi.org/10.1016/j.jclepro.2024.141906
134. Yu, Y., Liu, W., Zhang, Y., Zhang, B., Jin, Y., Chen, S., Tang, S., Su, Y., Yu, X., & Chen, G. (2024). Chitosan/magnetic biochar composite with enhanced reusability: Synergistic effect of functional groups and multilayer structure. Arabian Journal of Chemistry, 17, 105746. https://doi.org/10.1016/j.arabjc.2024.105746
135. Zhou J, He Y, Huang L, Xu A, Zhao Y, Wang J, He G, Fan S, Huang Z. Preparation of magnetic biochar from macadamia nutshell pretreated by FeCl3-assisted mechanochemical activation for adsorption of heavy metals. Journal of Environmental Chemical Engineering. 2024 Aug 1;12(4):113122. https://doi.org/10.1016/j.jece.2024.113122
136. Singh K, Azad SK, Dave H, Prasad B, Maurya DM, Kumari M, Dubey D, Rai AK, Sillanpää M, Sah MP, Prasad KS. Effective removal of Cr (VI) ions from the aqueous solution by agro-waste-based biochar: an exploration of batch and column studies. Biomass Conversion and Biorefinery. 2024 Aug;14(16):19215-29. https://doi.org/10.1007/s13399-023-04268-9
137. Zhao, H., Ma, F., Ren, X., Zhao, B., Jiang, Y., & Zhang, J. (2025). Green Synthesis of nZVI-Modified Sludge Biochar for Cr (VI) Removal in Water: Fixed-Bed Experiments and Artificial Neural Network Model Prediction. Water, 17(3), 341. https://doi.org/10.3390/w17030341
138. Zhang A, Li X, Xing J, Xu G. Adsorption of potentially toxic elements in water by modified biochar: A review. Journal of Environmental Chemical Engineering. 2020 Aug 1;8(4):104196. https://doi.org/10.1016/j.jece.2020.104196
139. Liang M, Ding Y, Zhang Q, Wang D, Li H, Lu L. Removal of aqueous Cr (VI) by magnetic biochar derived from bagasse. Scientific reports. 2020 Dec 8;10(1):21473. https://doi.org/10.1038/s41598-020-78142-3
140. Zuo J, Li W, Xia Z, Zhao T, Tan C, Wang Y, Li J. Preparation of modified biochar and its adsorption of Cr (VI) in aqueous solution. Coatings. 2023 Nov 2;13(11):1884. https://doi.org/10.3390/coatings13111884
141. Wang J, Guan Y, Fu J, Liu X, Guo M, Gao J, Yang M, Liu X, Jin Y, Qu J. Efficient chromium remediation using eco-innovative biochar in a novel two-stage upflow fixed bed system. Journal of Water Process Engineering. 2024 Nov 1; 67:106147. https://doi.org/10.1016/j.jwpe.2024.106147

 doi:10.20944/preprints202605.1519.v1

142. Ali A, Alharthi S, Al-Shaalan NH, Naz A, Fan HJ. Efficient removal of hexavalent chromium (Cr (VI)) from wastewater using amide-modified biochar. Molecules. 2023 Jun 30;28(13):5146. https://doi.org/10.3390/molecules28135146
143. Karthik V, Periyasamy S, Dharneesh S, Duvakeesh GK, Gizaw DG, Vijayashankar T. Biochar as a sustainable adsorbent for heavy metal removal from polluted waters: a comprehensive outlook. Journal of Chemistry. 2024;2024(1):8217730. https://doi.org/10.1155/joch/8217730
144. US Environmental Protection Agency. Method 1311: Toxicity Characteristic Leaching Procedure (SW 846). Washington (DC): US EPA; 1992.
145. Shen Z, Hou D, Zhao B, Xu W, Ok YS, Bolan NS, Alessi DS. Stability of heavy metals in soil washing residue with and without biochar addition under accelerated ageing. Science of the Total Environment. 2018 Apr 1; 619:185-93. https://doi.org/10.1016/j.scitotenv.2017.11.038
146. Long XX, Yu ZN, Liu SW, Gao T, Qiu RL. A systematic review of biochar ageing and the potential eco-environmental risk in heavy metal contaminated soil. Journal of Hazardous Materials. 2024 Jul 5; 472:134345. https://doi.org/10.1016/j.jhazmat.2024.134345
147. Wang L, O'Connor D, Rinklebe J, Ok YS, Tsang DC, Shen Z, Hou D. Biochar aging: mechanisms, physicochemical changes, assessment, and implications for field applications. Environmental Science & Technology. 2020 Nov 3;54(23):14797-814. https://doi.org/10.1021/acs.est.0c04033
148. Chang R, Sohi SP, Jing F, Liu Y, Chen J. A comparative study on biochar properties and Cd adsorption behaviour under effects of ageing processes of leaching, acidification and oxidation. Environmental pollution. 2019 Nov 1; 254:113123. https://doi.org/10.1016/j.envpol.2019.113123
149. International Organization for Standardization. ISO 6341:2012. Water quality — Determination of the inhibition of the mobility of Daphnia magna Straus (Cladocera, Crustacea) — Acute toxicity test. Geneva: ISO; 2012.
150. International Organization for Standardization. ISO 11348 3:2007. Water quality — Determination of the inhibitory effect of water samples on the light emission of Aliivibrio fischeri (Luminescent bacteria test) — Part 3: Method using freeze dried bacteria. Geneva: ISO; 2007.
151. Restrepo JB, Flohr L, Melegari SP, da Costa CH, Fuzinatto CF, de Castilhos AB, Matias WG. Correlation between acute toxicity for Daphnia magna, Aliivibrio fischeri and physicochemical variables of the leachate produced in landfill simulator reactors. Environ. Technol. 2017 Nov; 38:2898-906. https://doi.org/10.1080/09593330.2017.1281352
152. International Organization for Standardization. ISO 11269 1:2012. Soil quality — Determination of the effects of pollutants on soil flora — Part 1: Method for the measurement of inhibition of root growth. Geneva: ISO; 2012.
153. Di Salvatore M, Carafa AM, Carratu G. Assessment of heavy metals phytotoxicity using seed germination and root elongation tests: A comparison of two growth substrates. Chemosphere. 2008 Nov 1;73(9):1461-4. https://doi.org/10.1016/j.chemosphere.2008.07.061